

Agent Explorative Policy Optimization for Multimodal Agentic Reasoning

Minki Kang^{1,2*}, Shizhe Diao¹, Ryo Hachiuma¹, Sung Ju Hwang², Pavlo Molchanov¹, Yu-Chiang Frank Wang¹, Byung-Kwan Lee^{1†}

¹NVIDIA ²KAIST

Abstract

Vision-language models with extended reasoning succeed on complex problems, but many real-world problems require external tools that internal reasoning alone often cannot resolve. Agentic reasoning therefore interleaves two behaviors with a structural asymmetry: thinking (the self-contained default) and tool use (a high-variance auxiliary acting). We refer to this asymmetry as the *Thinking-Acting Gap*. Under standard RL recipes like GRPO, the gap manifests as two diagnostic symptoms during training: tool use is attempted on only $\sim 30\%$ of rollouts, and when attempted, the tool-using rollouts within a group are all-wrong on $\sim 40\%$ of questions, suppressing the learning signal at the tool calls that needed it. We propose **AXPO** (Agent eXplorative Policy Optimization): for each all-wrong tool-using subgroup, AXPO fixes the thinking prefix and resamples the tool call and its continuation, paired with uncertainty-based prefix selection. Across nine multimodal benchmarks and three scales of Qwen3-VL-Thinking, SFT + AXPO outperforms SFT + GRPO at average (+1.8 pp Pass@1 and +1.8 pp Pass@4 at 8B on average) and 8B with SFT + AXPO surpasses the 32B Base on Pass@4 with 4 \times fewer parameters. The project page is available at [link](#).

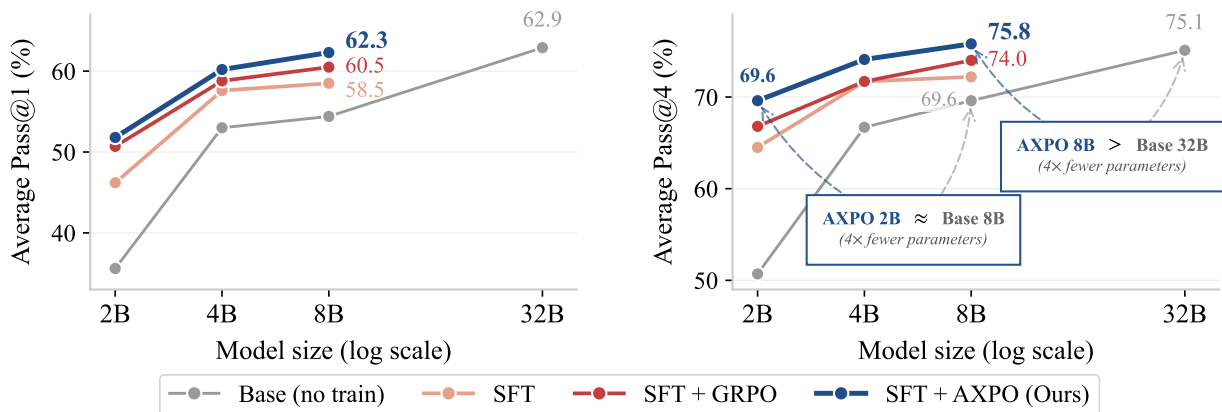


Figure 1 | **Main result: AXPO narrows the agentic gap to a 4 \times larger baseline.** Average Pass@1 (left) and Pass@4 (right) over nine multimodal benchmarks across Qwen3-VL-Thinking sizes. At 8B, AXPO surpasses the 32B Base baseline on Pass@4 while outperforming GRPO at every scale.

1. Introduction

Large language models (LLMs) and vision-language models (VLMs) with extended reasoning capabilities have made remarkable progress, producing chains of thought that rival much larger models on mathematical and scientific reasoning benchmarks [1–3]. These reasoning models invest test-time compute into internal search and reflection to arrive at accurate answers. However, many real-world problems lie beyond what internal reasoning alone can resolve: retrieving up-to-date knowledge, performing complex numerical computation, and understanding fine-grained visual details all require access to external resources [4–8]. Tools such as web search, code interpreters, and image manipulation utilities can fill this gap, enabling what we call **Multimodal Agentic Reasoning**: the model autonomously decides when to think further and when to act through tools, much as it

*Work done during internship. †Project Lead.

Correspondence to <minkikang@kaist.ac.kr, byungkwan1@nvidia.com>

© 2026 NVIDIA. All rights reserved.

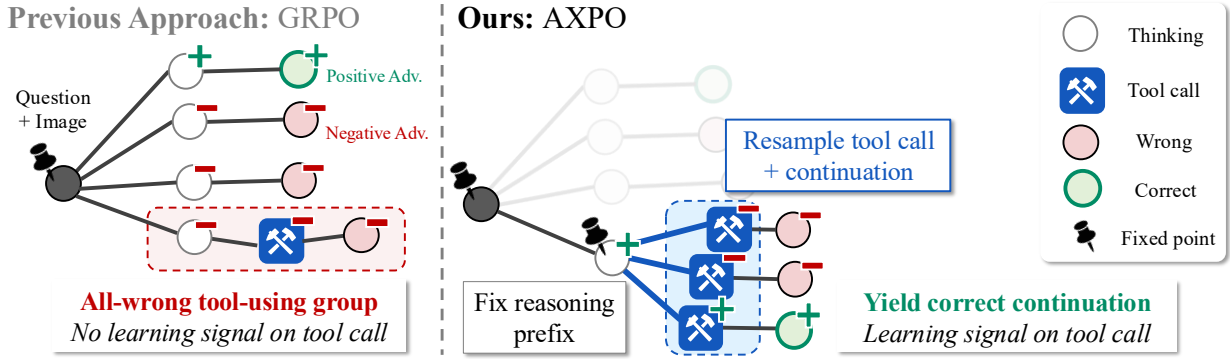


Figure 2 | **Concept.** AXPO concentrates exploration on the tool call for agentic reasoning. **Left:** under GRPO, tool-using rollouts are scarce and often fail, leaving no positive learning signal at the tool call where it is most needed. **Right:** AXPO fixes the thinking prefix from the failed rollout and resamples the tool call and its continuation, recovering a correct rollout and producing a positive learning signal on the tool call.

learns to allocate thinking budget, but now extended to interaction with environments [9–14].

Agentic reasoning carries a deeper asymmetry between its two constituent behaviors: *Thinking* and *Tool use (Acting)*. *Thinking* is the default mode, self-contained within the model’s token space: every token is under its control and errors can be corrected by exploring a different chain of thought [15–17]. *Tool use*, by contrast, is an auxiliary behavior that is simultaneously powerful but fragile: a short token sequence triggers an external response the model cannot predict or control, and small changes in the call can produce drastically different outcomes (e.g., invalid python code with wrong indent) [18]. Reasoning models are heavily post-trained for thinking, but far less for acting. We refer to this asymmetry between a safe default and a high-variance auxiliary as the **Thinking-Acting Gap**.

Due to this gap, eliciting agentic reasoning remains a challenge despite the capabilities of recent reasoning VLMs [19]. Relying solely on prompting is often insufficient to ensure an appropriate tool call when needed. This necessitates post-training pipelines, such as Supervised Fine-Tuning (SFT) and Reinforcement Learning (RL), as evidenced in Figure 1. SFT reliably teaches the *mechanics* of tool use but struggles to teach the model to utilize tools better for situations the teacher’s demonstrations did not cover. The resulting agent inherits the teacher’s failure modes and often plateaus near its performance [20, 21]. Therefore, the model requires a training signal that goes beyond imitation, which motivates utilizing RL with verifiable outcome rewards after SFT [18, 22, 23].

However, RL methods such as GRPO [24–26] are suboptimal to make models proficient at acting, because two patterns suppress the tool-call learning signal. First, tool use remains a minority of rollouts compared with thinking-only (Figure 3a). Second, when tool use is attempted, the entire group of rollouts is far more likely to fail together (Figure 3b). Under GRPO, this asymmetry weakens the tool-call learning signal in both regimes: tool-using rollouts trail thinking-only successes in mixed groups (negative advantage) and zero out in all-wrong groups [27, 28]. These observations motivate targeted exploration for tool use during RL. This raises a critical question: *how can we effectively induce such exploration?* The Thinking-Acting Gap suggests the answer. Thinking is the native mode of the model and the tool call is the separate mode that turns an intent into a concrete action where the same intent admits diverse implementations (Figure 3c).

Building on this observation, our key insight is that resampling at the tool call lets the model explore diverse agentic reasoning: we anchor the thinking prefix and resample the tool call and its continuation (Figure 2). We call this *tool-call resampling*. The operation has no analog in pure reasoning, where there is no comparable boundary between a committed intent and a high-variance

action. When a tool-using trajectory fails, the thinking prefix may be entirely sound. Re-deriving the full trajectory from scratch wastes budget on prefixes that were not the bottleneck, whereas tool-call resampling concentrates exploration precisely where the Thinking-Acting Gap manifests. We propose **AXPO** (Agent eXplorative Policy Optimization) based on this principle to narrow the gap during RL.

Concretely, AXPO instantiates three design choices on top of a small extra rollout budget: (1) *where to resample*, only on all-wrong tool-using subgroups where a single recovery flips the GRPO advantage; (2) *which prefix*, the highest-uncertainty ones; and (3) *how resamples enter the gradient*, a per-prefix GRPO advantage on continuations and a binary recovery indicator on the source prefix. Unlike prior reward-shaping methods [18, 23, 29] or rollout scaling methods [30, 31], AXPO restructures the rollout distribution itself at the locus of the Thinking-Acting Gap.

Across nine multimodal benchmarks at Qwen3-VL-Thinking 2B/4B/8B [19], SFT + AXPO outperforms SFT + GRPO at average with Pass@4 gains of +2.8/+2.3/+1.8 pp. **At 8B, SFT + AXPO surpasses the 32B Base** on Pass@4 and reaches 99% of its Pass@1, despite using 4× fewer parameters (Figure 1). The improvement concentrates on tool-intensive benchmarks, while preserving the performance improvement in reasoning benchmarks compared to SFT + GRPO baseline. Notably, +25% extra resampling budget with AXPO delivers +1.1 pp over +100% extra rollout budget with GRPO, confirming that the gain comes from where compute is spent.

Our contributions are as follows:

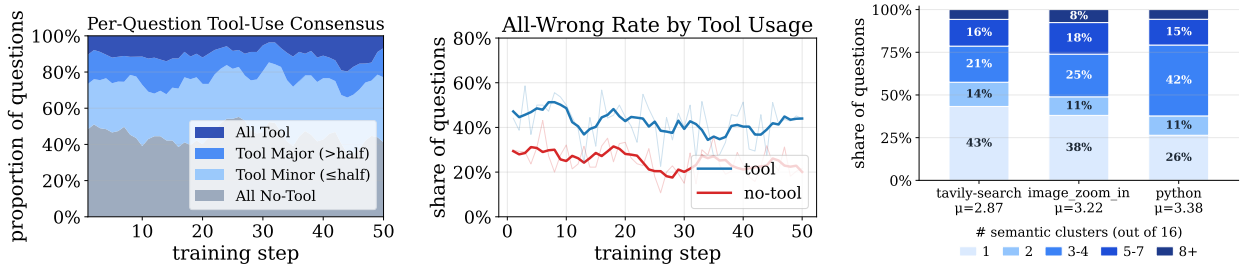
- We identify the **Thinking-Acting Gap**, an asymmetry between thinking and tool use that manifests in group-based agentic RL as two symptoms: tool use is attempted on 30% of rollouts and tool-using subgroups (the tool-using rollouts within a group) are all-wrong on 40% of questions, yielding non-positive advantage on tool-call tokens.
- We propose **AXPO**, an RL algorithm that closes the gap via *tool-call resampling*: for all-wrong tool-using subgroups, AXPO fixes the thinking prefix at uncertain tool calls and resamples from them, provably dominating from-scratch sampling on tool-use coverage at fixed budget.
- We validate AXPO on nine multimodal benchmarks across three scales of Qwen3-VL-Thinking, with gains for all sizes compared to GRPO baseline, and the **resulting 2B model matches the 8B Base and the 8B model surpasses the 32B Base on Pass@4**.

2. Analysis of RL in Agentic Reasoning

2.1. Preliminaries

Agentic Reasoning. We study the agentic reasoning of Vision-Language Models (VLMs) π_θ given an input \mathbf{x} (text question with visual image) and instruction prompt (A.2), interleaving thinking and tool use. At turn t , the model emits a thinking segment \mathbf{t}_t (in `<think> ...</think>`) and an action \mathbf{a}_t (a tool call formatted as JSON with tool type and arguments, in `<tool_call> ...</tool_call>`), then receives an observation $\mathbf{o}_t = \text{exec}(\mathbf{a}_t)$ (in `<tool> ...</tool>`). We write $\mathbf{y}_t = \mathbf{t}_t\mathbf{a}_t\mathbf{o}_t$ with $\mathbf{t}_t\mathbf{a}_t \sim \pi_\theta(\cdot \mid \mathbf{x}, \mathbf{y}_{<t})$. This continues until the final answer (in `<answer> ...</answer>`) is emitted or the turn limit is reached, yielding $\tau = (\mathbf{x}, \mathbf{y}_1, \dots, \mathbf{y}_T, \mathbf{y}_{\text{ans}})$. Our tool set covers three standard [7, 18, 23]: a Python interpreter, a web search, and an image zoom-in tool.

RL training with GRPO. Our starting point is the standard agentic post-training pipeline [18, 23]: supervised fine-tuning (SFT) on expert trajectories followed by reinforcement learning (RL) with verifiable rewards. Given an input \mathbf{x} , the policy π_θ generates a group of N rollouts $\{\tau_i\}_{i=1}^N$, each receiv-



(a) Proportion of questions by tool- (b) All-wrong rate by subgroup type (c) Semantic cluster count of 16 using rollout count (8 rollouts/ques- under GRPO: the tool-using fails resampled tool calls from a fixed tion) across RL steps under GRPO. together far more than the no-tool. failed-rollout prefix, per tool type.

Figure 3 | **Empirical analysis of diagnosing the Thinking-Acting Gap** (Section 2.2). (a) Tool use is under-attempted. (b) The tool-using subgroup (the tool-using rollouts within a GRPO group) fails all-together far more often than the no-tool subgroup. (c) Resampling at a fixed prefix preserves substantive diversity in the tool call, confirming it as a real divergence point.

ing a binary outcome reward $r_i \in \{0, 1\}$ based on answer correctness. Group Relative Policy Optimization (GRPO) [24] computes a group-normalized advantage $A_i = (r_i - \text{mean}(\{r_j\}_{j=1}^N)) / \text{std}(\{r_j\}_{j=1}^N)$, which is assigned uniformly to every token in τ_i and used to update the policy via the PPO-clip surrogate $\mathcal{L}_{\text{clip}}$ [32]. We defer the explicit form of $\mathcal{L}_{\text{clip}}$ in Appendix A.1.

2.2. Diagnosing the Thinking-Acting Gap

We now ground the Thinking-Acting Gap in three diagnostic measurements collected during RL training (Figure 3). Our starting point is the SFT checkpoint, trained with GRPO [24] on outcome rewards.

Tool use is under-attempted. A defining property of agentic reasoning, unlike conventional agentic RL [31, 33], is that tool use is *optional*: the model can either produce a `<tool_call>` tag or skip straight to `<answer>`. This optionality makes action fragile under RL. We track the fraction of rollouts that contain at least one tool call over the course of RL. As shown in Figure 3a, which bins each question by its tool-using rollout count among $N = 8$, the corresponding rollout-level tool-use rate is roughly 27% at step 1 and stays in the 20–35% range over RL training, well below the thinking-only majority. GRPO exerts no pressure to grow the tool-using minority, and the behavior that distinguishes agentic from non-agentic reasoning remains under-represented in each group.

When attempted, the tool-using subgroup is prone to being all-wrong. Within a GRPO group of N rollouts for one question, we call the rollouts that emit a tool call the *tool-using subgroup* and the rest the *no-tool subgroup*, and the tool-using subgroup is *all-wrong* when none of its rollouts is correct, even if some no-tool rollouts in the same group succeed. Conditional on a question where tool use is attempted, how often does the tool-using subgroup fail together? Figure 3b shows this all-wrong rate is $\sim 40\%$ for tool-using subgroups compared to $\sim 25\%$ for no-tool subgroups. Under group-normalized advantage, this asymmetry yields non-positive advantage on tool-call tokens in both regimes: in mixed groups they trail the no-tool success signal, and in fully all-wrong groups the numerator $r_i - \text{mean}(\{r_j\})$ collapses to zero. Either way, effective learning signal on tool calls is suppressed on the questions where tool use would matter most.

Tool calls admit substantive resampling at a fixed thinking. Resampling at the tool call is only worthwhile if it is a real divergence point under the policy. If the thinking prefix already

commits to the concrete action, resampling at the tool-call boundary changes nothing. We probe this by decomposing a trajectory at the first tool-call boundary: we fix its thinking prefix \mathbf{t}_1 , draw 16 continuations from $\pi_\theta(\cdot \mid \mathbf{x}, \mathbf{t}_1)$, and cluster the resulting tool calls into semantic classes by an LLM judge that groups calls by their semantic intent. Figure 3c shows that the resampled tool calls do not collapse to a single class. Across all tools, the 16 samples occupy 2.9–3.4 distinct semantic clusters on average. The thinking prefix therefore does not determine the exact tool call and the tool call is an under-explored divergence point whose exploration must be supplied externally.

Takeaways: GRPO under-trains the tool call

- Tool use remains a minority behavior under GRPO: $\sim 20\text{--}35\%$ of rollouts across RL steps, well below the thinking-only majority (Figure 3a).
- When attempted, the tool-using subgroup is all-wrong on $\sim 40\%$ of questions (vs. 25% for the no-tool subgroup), so tool-call tokens get negative advantage in mixed groups and zero in fully all-wrong groups (Figure 3b).
- Resampling from a fixed prefix preserves substantive diversity in the tool call (2.9–3.4 semantic clusters per 16 samples in Figure 3c): the tool call is a real divergence point.

3. Agent eXplorative Policy Optimization (AXPO)

3.1. Tool-call resampling

In agentic reasoning, the policy must learn both thinking and tool use where the latter is the under-trained behavior under GRPO (Section 2.2). Rather than scaling rollouts N to generate tool-using successes uniformly, we commit to a thinking prefix that promises a tool call and concentrate stochasticity on the continuation.

Concretely, let τ^{src} denote a **tool-using** rollout from the standard GRPO group of \mathbf{x} , which we call the *source rollout*, and let $\mathbf{t}_1^{\text{src}}$ be its prefix that includes the opening `<tool_call>` tag, so that decoding from $\mathbf{t}_1^{\text{src}}$ is constrained to produce a valid tool call. *Tool-call resampling* draws K continuations $\{\mathbf{y}_k^{\text{res}}\}_{k=1}^K \sim \pi_\theta(\cdot \mid \mathbf{x}, \mathbf{t}_1^{\text{src}})$, executes the tool calls inside each, and rolls every resampled trajectory forward until an `<answer>` tag or the turn limit. Each resampled trajectory $\tau_k^{\text{res}} = (\mathbf{t}_1^{\text{src}}, \mathbf{y}_k^{\text{res}})$ therefore shares the fixed thinking prefix with τ^{src} and diverges at the tool call, concentrating stochasticity on the action that the thinking was preparing for. Each resampled trajectory receives the same binary outcome reward $r_k^{\text{res}} \in \{0, 1\}$ as a standard rollout.

Theoretical motivation. *Why grow tool-using rollout coverage?* Recent analysis [30] shows that scaling per-prompt rollouts N yields a policy-improvement guarantee that grows with the correct-token mass the group covers. However, our learning target is correct *tool-using* rollouts carry positive gradient signal for tool-call tokens, so coverage at the tool call is bounded by the tool-use rate $q = \Pr_{\pi_\theta}[\text{tool use} \mid \mathbf{x}]$ rather than N , and a fraction $1 - q$ of any raw sampling budget is wasted on non-tool rollouts that cannot teach the tool call. Tool-call resampling sidesteps this waste by committing to a prefix $\mathbf{t}_1^{\text{src}}$ that has already crossed the `<tool_call>` boundary: every resampled continuation from $\mathbf{t}_1^{\text{src}}$ is tool-using by construction, so the full resampling budget lands on the signal we actually want.

Let $p(\mathbf{t}_1^{\text{src}}) = \Pr_{\pi_\theta}[R = 1 \mid \mathbf{x}, \mathbf{t}_1^{\text{src}}]$ be the success probability of a continuation from prefix $\mathbf{t}_1^{\text{src}}$, and $p^{\text{tool}} = \Pr_{\pi_\theta}[R = 1 \mid \mathbf{x}, \text{tool use}]$ the per-tool-using-rollout success rate of standard rollout. The following proposition makes the gain precise.

Proposition 1 (Tool-call resampling dominates raw sampling at recovering tool-using successes).

Let $\mathbf{t}_1^{\text{src}}$ be a prefix that has crossed the tool call boundary with $p(\mathbf{t}_1^{\text{src}}) \geq qp^{\text{tool}}$. Then for any $N \geq 1$,

$$\underbrace{1 - (1 - p(\mathbf{t}_1^{\text{src}}))^N}_{\text{resampling: } N \text{ tool-using continuations}} \geq \underbrace{1 - (1 - qp^{\text{tool}})^N}_{\text{raw: } N \text{ rollouts, } q\text{-fraction tool-using}}, \quad (1)$$

with strict inequality whenever $p(\mathbf{t}_1^{\text{src}}) > qp^{\text{tool}}$ and $qp^{\text{tool}} \in (0, 1)$. Both sides measure the probability that the group contains at least one correct tool-using rollout.

The key mechanism is $q \rightarrow 1$ by construction: every resampled continuation from $\mathbf{t}_1^{\text{src}}$ is tool-using, so $(1 - q)$ waste factor vanishes and the threshold qp^{tool} sits strictly below the average per-tool-using-rollout success p^{tool} , admitting prefixes at or below the conditional mean. Under GRPO, the left-hand side equals the probability that the tool-using subgroup produces a positive gradient, so resampling strictly raises the probability of recovering an all-wrong tool-using subgroup identified in [Section 2.2](#) relative to raw sampling at any fixed N . Detailed analysis is in [Appendix D](#).

3.2. Resample candidate selection

Trigger and budget allocation. AXPO resamples only on groups in which the tool-using subgroup is non-empty and entirely wrong (an *all-wrong tool-using subgroup*; no-tool rollouts in the same group may succeed). These are exactly the groups where tool-call tokens receive non-positive advantage under GRPO ([Section 2.2](#)): zero when the entire group is all-wrong, negative when only no-tool rollouts succeed. A recovered continuation therefore delivers the largest gradient lift per resampled continuation. [Proposition 1](#) would in principle admit groups with at least one correct tool-using rollout as well, but those already produce positive advantage on tool-call tokens and gain comparatively little from a marginal recovery. Resampling every triggered prefix would add up to BNK continuations on top of BN standard rollouts (batch size B), so AXPO caps the extra cost up to $r \cdot BN$ per step with $r < 1$ and allocates breadth-first: every triggered question receives its top-ranked prefix before any receives a second.

Uncertainty-based prefix ranking. Not every admitted prefix is worth resampling. [Figure 3c](#) shows $\sim 30\%$ of prefixes collapse to a single cluster across 16 resamples. AXPO therefore ranks candidates by the mean policy probability over the tool-call tokens in τ^{src} (a tractable uncertainty proxy [\[34\]](#)) and resamples the lowest-confidence prefixes first (see [Appendix B.9](#) for the choice of confidence over predictive entropy).

3.3. Advantage calculation

Given the resampled trajectories from [Section 3.2](#), we now specify how their advantages enter the gradient. Because each τ_k^{res} shares its prefix with the source rollout τ^{src} , training both as independent rollouts would assign contradictory advantages to the prefix tokens: the failed source penalizes the prefix while a successful resample rewards it. AXPO decomposes the advantage streams so that every token is updated from exactly one source.

For each selected prefix $\mathbf{t}_1^{\text{src}}$, the K resampled continuations form an independent advantage group. We compute a per-prefix GRPO advantage

$$\hat{A}_k^{\text{res}}(\mathbf{t}_1^{\text{src}}) = \frac{r_k^{\text{res}} - \text{mean}(\{r_j^{\text{res}}\}_{j=1}^K)}{\text{std}(\{r_j^{\text{res}}\}_{j=1}^K)}, \quad k = 1, \dots, K, \quad (2)$$

which is applied only to the continuation tokens $\mathbf{y}_k^{\text{res}}$ where the prefix thinking tokens are masked. The source trajectory’s prefix tokens are updated through τ^{src} with a binary recovery reward that

fires whenever resampling recovers at least one correct continuation:

$$r^{\text{prefix}}(\mathbf{t}_1^{\text{src}}) = \mathbb{1}[\exists k \in \{1, \dots, K\} : r_k^{\text{res}} = 1]. \quad (3)$$

This recovery reward replaces the original (zero) source-rollout reward in the source group’s GRPO normalization, yielding a per-prefix advantage that we apply to the source’s prefix tokens as follows:

$$\hat{A}^{\text{prefix}}(\mathbf{t}_1^{\text{src}}) = \frac{r^{\text{prefix}}(\mathbf{t}_1^{\text{src}}) - \text{mean}(\{\tilde{r}_j\}_{j=1}^N)}{\text{std}(\{\tilde{r}_j\}_{j=1}^N)}, \quad \tilde{r}_j = \begin{cases} r^{\text{prefix}}(\mathbf{t}_1^{\text{src}}), & j = \text{source index,} \\ r_j, & \text{otherwise,} \end{cases} \quad (4)$$

and the source continuation is masked. Combining both streams with the standard clipped surrogate from PPO [32] yields the resampling contribution for a selected prefix $\mathbf{t}_1^{\text{src}}$ to maximize:

$$\mathcal{L}_{\text{AXPO}}(\mathbf{t}_1^{\text{src}}) = \underbrace{\mathcal{L}_{\text{clip}}(\mathbf{t}_1^{\text{src}}; \hat{A}^{\text{prefix}}(\mathbf{t}_1^{\text{src}}))}_{\text{prefix, source only}} + \sum_{k=1}^K \underbrace{\mathcal{L}_{\text{clip}}(\mathbf{y}_k^{\text{res}}; \hat{A}_k^{\text{res}}(\mathbf{t}_1^{\text{src}}))}_{\text{resampled continuation}}. \quad (5)$$

Non-triggered groups and rollouts not selected for resampling retain the standard GRPO loss from Section 2.1. Equation 5 is added once per prefix selected in Section 3.2. The recovery-indicator r^{prefix} avoids the gradient conflict of propagating mixed-sign continuation advantages back to the shared prefix: \hat{A}^{prefix} is monotone in r^{prefix} , so the prefix is credited positively whenever at least one continuation succeeds, converting the coverage gain into gradient signal on the prefix tokens.

4. Experiments

4.1. Experimental setup

Base models and tools. We use Qwen3-VL-Thinking [19] at three sizes (2B, 4B, 8B) as the base model across all methods. The tool set is the three families introduced in Section 2.1: a Python interpreter, a web search engine (Tavily search API¹), and an image zoom-in tool. All tools share a unified `<tool_call>` interface. Full prompt templates and tool schemas are in Appendix A.2.

Training data & pipeline. SFT uses 64K correct trajectories drawn from ViRL [35], fvqa [36], and PyVision-RL [18], generated by Qwen3-VL-32B-Thinking [19] where $\sim 25\%$ contain a tool call. RL uses a 16K filtered subset plus 22K questions from MMFineReason-hard [37]. We follow the SFT then RL pipeline of Section 2.1. AXPO augments the rollout loop with tool-call resampling, holding all other hyperparameters constant against SFT + GRPO. Full details are in Appendix A.1.

Benchmarks and metrics. We evaluate on nine multimodal benchmarks grouped into three task categories: **Reasoning** (MathVision [38], DynaMath [39], Math-VR [40]), **Perception** (V* [8], VisualProbe [7], HR-Bench-4K and HR-Bench-8K [41]), and **Search** (HR-MMSearch [42], MM-Search [43]); per-benchmark descriptions in Appendix A.3. All benchmarks are evaluated in the agentic setting with the same tool interface used in training. We report Pass@1 and Pass@4 (%), averaged over four rollouts per question, with answer matching logic tailored for each benchmark.

Baselines. We compare AXPO against four baselines: (1) **Base**: the base model only with prompting without additional training (2) **SFT**: the SFT checkpoint without RL (3) **GRPO**: RL from the base model without an SFT stage and (4) **SFT + GRPO**: the standard SFT-then-RL recipe. Our method, **SFT + AXPO**: applies tool-call resampling and advantage calculation from Section 3 on top of the same SFT-then-RL pipeline.

¹<https://www.tavily.com/>

Table 1 | Main results — Pass@1 (% , \uparrow) on **nine multimodal benchmarks**, grouped into three categories: Reasoning, Perception, and Search. All methods use **Qwen3-VL-Thinking** [19] at four sizes (2B, 4B, 8B, 32B). Best result per column within each size block is **bolded**; second-best is underlined. Δ rows show AXPO’s gain over SFT + GRPO, the strongest comparable training recipe where AXPO outperforms it in most of evaluations. Pass@4 results are reported in Table 5.

Method	Reasoning			Perception				Search		Avg.
	Math Vision	Dyna Math	Math -VR	V*	Visual Probe	HRBen. -4K	HRBen. -8K	HR-MM Search	MM Search	
<i>Qwen3-VL-2B-Thinking</i>										
Base	18.6	60.5	16.9	63.0	5.0	64.6	55.9	8.2	27.7	35.6
GRPO	33.7	64.9	34.6	67.1	23.8	65.0	59.4	18.4	41.4	45.4
SFT	28.9	64.1	30.2	75.9	24.5	73.1	68.8	14.5	35.9	46.2
+ GRPO	<u>34.8</u>	<u>66.4</u>	<u>35.8</u>	81.7	36.1	<u>74.3</u>	<u>70.6</u>	15.7	<u>40.6</u>	<u>50.7</u>
+ AXPO (Ours)	35.0	66.9	38.9	<u>81.3</u>	<u>35.1</u>	77.9	72.4	<u>18.1</u>	40.3	51.8
Δ vs. SFT + GRPO	+0.2	+0.5	+3.1	-0.4	-1.0	+3.6	+1.8	+2.4	-0.3	+1.1
<i>Qwen3-VL-4B-Thinking</i>										
Base	48.0	<u>76.6</u>	50.8	80.6	24.8	73.6	67.5	16.9	37.8	53.0
GRPO	<u>52.5</u>	76.2	57.9	82.7	29.7	75.5	71.1	12.7	23.8	53.6
SFT	49.1	76.3	55.3	87.0	34.7	<u>79.5</u>	<u>74.1</u>	20.6	41.5	57.6
+ GRPO	51.6	77.2	57.4	90.2	<u>38.0</u>	78.8	73.8	20.0	<u>42.3</u>	<u>58.8</u>
+ AXPO (Ours)	52.8	76.4	57.2	<u>88.9</u>	43.6	80.9	78.3	<u>20.1</u>	43.3	60.2
Δ vs. SFT + GRPO	+1.2	-0.8	-0.2	-1.3	+5.6	+2.1	+4.5	+0.1	+1.0	+1.4
<i>Qwen3-VL-8B-Thinking</i>										
Base	47.1	75.9	54.9	77.7	31.8	72.8	66.1	21.0	42.7	54.4
GRPO	54.4	77.2	58.9	85.7	<u>40.1</u>	77.1	73.9	20.6	45.1	59.2
SFT	50.9	76.8	58.4	84.8	38.4	<u>79.5</u>	74.4	23.0	40.6	58.5
+ GRPO	<u>55.3</u>	<u>78.2</u>	<u>60.4</u>	<u>87.7</u>	<u>40.1</u>	<u>79.5</u>	<u>74.9</u>	<u>24.4</u>	44.0	<u>60.5</u>
+ AXPO (Ours)	56.1	79.0	60.6	87.8	45.8	83.3	77.0	25.9	<u>45.0</u>	62.3
Δ vs. SFT + GRPO	+0.8	+0.8	+0.2	+0.1	+5.7	+3.8	+2.1	+1.5	+1.0	+1.8
<i>Qwen3-VL-32B-Thinking (inference-only baseline)</i>										
Base	56.5	83.3	64.1	89.1	40.3	85.3	78.9	22.8	46.1	62.9

4.2. Main Results: AXPO narrows the agentic gap to a 4 \times larger baseline.

Table 1 reports Pass@1 across nine benchmarks at four model sizes (per-benchmark Pass@4 results in Table 5, Appendix B.2). SFT + AXPO outperforms SFT + GRPO at average performance on Pass@1 (+1.1 / +1.4 / +1.8 pp at 2B/4B/8B). On Pass@4, SFT + AXPO also beats SFT + GRPO at every scale (+2.8 / +2.3 / +1.8 pp). **At 8B, SFT + AXPO reaches 99% of the 32B Base’s Pass@1 and surpasses it on Pass@4 (75.8 vs. 75.1), despite having 4 \times fewer parameters.** AXPO is the only recipe whose 8B point reaches the 32B line on Pass@1, and the only one whose Pass@4 crosses it (Figure 1).

Decomposing the 8B Pass@1 column of Table 1, SFT + AXPO gains +0.6 pp on Reasoning, +2.9 pp on Perception, and +1.3 pp on Search over the SFT + GRPO baseline. In relative terms, the gain concentrates in Perception (+4%) and is smallest on Reasoning (+1%). Perception is where image-tool use most directly determines correctness, while on Reasoning the bottleneck is often the thinking rather than the tool call. A detailed discussion of the results is provided in Appendix B.4.

4.3. Ablations: All components of AXPO matter

Table 2 ablates each AXPO design choice on 8B. Every component contributes: removing prefix fixing, the resampling target, uncertainty-based prefix selection, prefix credit, or the per-prefix

Table 2 | **AXPO ablations on Qwen3-VL-8B-Thinking**. Each row removes (or alters) one AXPO design choice from the full method. All rows share the SFT initialization. Best per column is **bolded**; second-best underlined.

Method	MathVision		V*		VisualProbe		HR-MMSearch		Average	
	P@1	P@4	P@1	P@4	P@1	P@4	P@1	P@4	P@1	P@4
SFT +										
AXPO w/o prefix fix (rollout from scratch)	56.0	75.0	86.9	96.9	43.6	68.9	<u>21.9</u>	35.7	<u>52.1</u>	<u>69.1</u>
w/ no-tool rollout resampling	54.9	71.4	89.1	<u>96.3</u>	41.5	62.3	21.1	33.4	51.7	65.9
w/o uncertainty rank	53.0	72.4	85.7	93.2	<u>43.9</u>	63.2	21.4	34.4	51.0	65.8
w/o prefix credit	<u>57.2</u>	76.6	86.3	95.3	40.6	62.3	21.6	<u>36.7</u>	51.4	67.7
w/o separated advantage group	57.7	76.6	87.2	95.8	40.1	61.3	19.8	34.4	51.2	67.0
AXPO (Ours)	56.1	<u>75.7</u>	<u>87.8</u>	95.3	45.8	<u>67.9</u>	25.9	42.0	53.9	70.2

Table 3 | **Comparison to alternative RL recipes on Qwen3-VL-8B-Thinking**. All rows share the SFT initialization. *Reward shaping & sampling* adds a per-tool-call reward or doubles the GRPO rollout budget. *RL algorithms* replaces GRPO with another alternative. Best per column is **bolded**; second-best underlined.

Method	MathVision		V*		VisualProbe		HR-MMSearch		Average	
	P@1	P@4	P@1	P@4	P@1	P@4	P@1	P@4	P@1	P@4
SFT +										
GRPO (baseline)	55.3	<u>75.0</u>	87.7	96.9	40.1	63.2	<u>24.4</u>	<u>38.0</u>	51.9	<u>68.3</u>
<i>Reward shaping & sampling</i>										
GRPO + Tool penalty [29]	53.0	69.7	83.1	90.1	30.4	46.2	17.4	30.5	46.0	59.1
+ Tool bonus [18, 44, 45]	52.9	72.7	86.0	93.2	42.7	59.4	21.6	37.0	50.8	65.6
+ rollout 2× (compute 2×)	<u>55.6</u>	73.4	87.0	<u>95.8</u>	<u>43.6</u>	<u>67.0</u>	23.2	36.7	<u>52.4</u>	68.2
<i>RL algorithms</i>										
RLTF [46]	42.4	65.5	79.8	84.3	30.2	42.5	20.6	31.8	43.3	56.0
CISPO [47]	54.3	71.1	86.0	93.7	29.2	48.1	21.5	35.7	47.8	62.2
ARPO [31]	53.2	71.7	89.3	<u>95.8</u>	41.0	60.4	21.6	34.4	51.3	65.6
AXPO (Ours)	56.1	75.7	<u>87.8</u>	95.3	45.8	67.9	25.9	42.0	53.9	70.2

advantage group all degrade both Pass@1 and Pass@4 average. Per-row analysis is in [Appendix B.6](#).

4.4. AXPO outperforms alternative RL recipes

[Table 3](#) compares AXPO against alternative training recipes: reward shaping (tool penalty / bonus), an extra rollout budget, and other RL algorithms (RLTF [46], CISPO [47], ARPO [31]). AXPO exceeds every alternative on both Pass@1 and Pass@4. The most direct more compute control, rollout 2×, doubles rollout budget yet underperforms than AXPO. The gain therefore comes from *where* compute is spent, not from *how much*. Reward-shaping methods both fall below the GRPO baseline of 51.9, indicating the gap is not closed by reward shaping either in agentic reasoning. Detailed analysis is in [Appendix B.7](#).

4.5. AXPO narrows the Thinking-Acting Gap during RL

Training dynamics. [Figure 4](#) (left & middle) tracks the two diagnostic symptoms of [Section 2.2](#) over RL steps. Under SFT + GRPO, the tool-use rate stays flat near ~30% and the all-wrong rate hovers around ~40% throughout training. Under SFT + AXPO, tool-use climbs +28 pp over training and the all-wrong rate sits ~17 pp below GRPO at *every* step, with tool-use rising during AXPO training while the all-wrong rate is suppressed by branching at each step, both consistent only under AXPO. The AXPO all-wrong rate is measured on the post-resampling subgroup composition (a tool-using subgroup that resampling recovers with at least one correct continuation no longer counts as all-wrong), so this persistent middle-panel gap is the per-step restore rate visualized in the right panel: tool-call resampling flips ~12% of all-wrong tool-using subgroups per step into subgroups

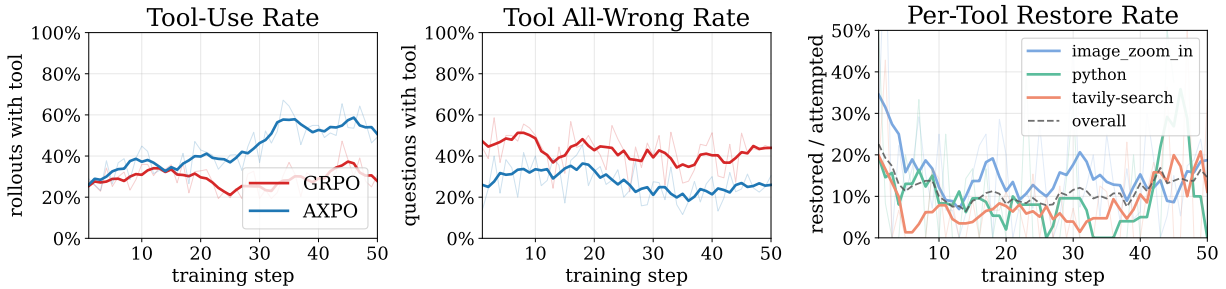
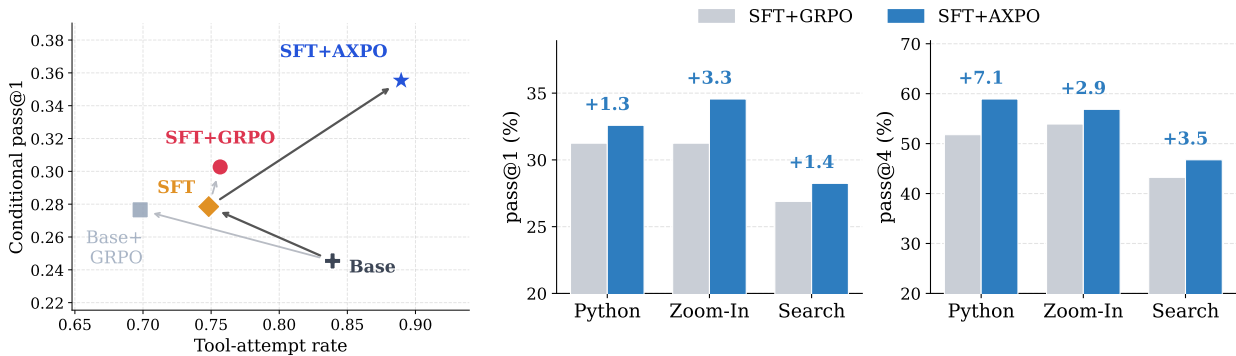


Figure 4 | Both Thinking-Acting Gap symptoms reverse during AXPO training but stay flat under GRPO, and the recovery does happen at resampling. **Left & Middle:** tool-use rate (top) and all-wrong rate on tool-using subgroups (bottom) over RL steps. **Right:** per-tool failed-subgroup recovery rate — the share of all-wrong tool-using subgroups that resampling flips into a subgroup with at least one correct tool-using trajectory.



(a) Training stages on the tool-attempt rate vs. conditional pass@1 plane. Only AXPO improves pass@1 and pass@4 across all three tool families. AXPO expands both axes simultaneously. (b) Per-tool quality on the matched-tool-use subset (questions with at least one correct tool-call continuation). This rate is non-trivial because resampling targets the hardest cases where every original tool-using rollout already failed, and restores learning signal so the policy is rewarded for tool use.

Figure 5 | **Post-training analysis** pooled over MathVision, VisualProbe-Hard, and HR-MMSearch on 8B model. Conditional Pass@1 is measured on 715 tool-attempted questions from each benchmark.

with at least one correct tool-call continuation. This rate is non-trivial because resampling targets the hardest cases where every original tool-using rollout already failed, and restores learning signal so the policy is rewarded for tool use.

Test-time dynamics. More globally, Figure 5a positions each training stage on the (tool-attempt rate, conditional Pass@1) plane measured on three benchmarks: every other stage either trades tool frequency for quality (Base \rightarrow GRPO or SFT) or holds tool frequency fixed while pushing only quality (SFT \rightarrow SFT + GRPO), while **only SFT + AXPO advances along both axes simultaneously**. The post-training matched-tool analysis (Figure 5b) is the per-question analysis of this joint advance: on questions where SFT + GRPO and SFT + AXPO both invoke a tool, AXPO improves Pass@1 across all three tool families, indicating the gain is in tool interaction quality.

5. Related Works

Agentic reasoning for VLMs. Agentic reasoning extends the reasoning loop beyond the model’s token space, allowing it to emit a tool call, receive an external output, and condition subsequent reasoning on it [48, 9]. Tools span knowledge search [5, 4], computation [10, 11, 49–51], and visual perception [44, 7, 12, 45, 52, 53]. Recent VLM systems combine image manipulation with code and search [43, 23, 18, 14, 54], and follow a two-stage SFT-then-RL recipe.

RL for agentic reasoning. On thinking-only trajectories, group-relative methods like GRPO [24–26] normalize rewards within N rollouts and uniformly assign the resulting advantage; BroRL [30] analyzes how scaling N closes coverage gaps. Three lines extend this family to tool-using rollouts: *direct ports* that reuse outcome-reward RL without changing the sampling structure [45, 23, 55–58, 22, 42], *mid-trajectory branching* that resamples the continuation after a tool call to absorb tool-output uncertainty [31, 59], and *reward shaping* that adds bonus or penalty terms on tool use [18, 29]. We include more detailed comparison with related works in [Appendix C](#).

Our contribution. AXPO contrasts with each line. Against direct use of GRPO, it restores learning signal on the all-wrong tool-using subgroups identified in [Section 2.2](#), which uniform sampling cannot reach. Against mid-trajectory branching [31, 59], it resamples *at* the tool-call boundary rather than after the tool observation, exploring the tool call itself rather than the continuation given a tool output. Against reward shaping, it acts on the rollout distribution while leaving the reward intact.

6. Conclusion

We identified a *Thinking-Acting Gap* in group-based agentic RL, an asymmetry between thinking (the self-contained default) and tool use (a high-variance auxiliary) that manifests during training as two symptoms: tool use is attempted on a minority of rollouts and tool-using subgroups (the tool-using rollouts within a group) are disproportionately all-wrong, so the advantage at tool-call tokens is non-positive on exactly the questions where tool use would help. AXPO narrows this gap by augmenting the rollout loop with *tool-call resampling*, which fixes the thinking prefix and concentrates exploration on the tool call itself, paired with uncertainty-based prefix selection. Across nine multimodal benchmarks and three model scales, AXPO consistently outperforms SFT + GRPO, and at 8B it surpasses the 32B Base baseline on Pass@4 with 4× fewer parameters.

Limitations. Our study assumes verifiable outcome rewards for RL and trains models up to 8B parameters. We discuss limitations and the future directions in details in [Appendix E](#).

References

- [1] DeepSeek-AI, Daya Guo, Dejian Yang, Haowei Zhang, Junxiao Song, Ruoyu Zhang, Runxin Xu, Qihao Zhu, Shirong Ma, Peiyi Wang, Xiao Bi, Xiaokang Zhang, Xingkai Yu, Yu Wu, Z. F. Wu, Zhibin Gou, Zhihong Shao, Zhuoshu Li, Ziyi Gao, Aixin Liu, Bing Xue, Bingxuan Wang, Bochao Wu, Bei Feng, Chengda Lu, Chenggang Zhao, Chengqi Deng, Chenyu Zhang, Chong Ruan, Damai Dai, Deli Chen, Dongjie Ji, Erhang Li, Fangyun Lin, Fucong Dai, Fuli Luo, Guangbo Hao, Guanting Chen, Guowei Li, H. Zhang, Han Bao, Hanwei Xu, Haocheng Wang, Honghui Ding, Huajian Xin, Huazuo Gao, Hui Qu, Hui Li, Jianzhong Guo, Jiashi Li, Jiawei Wang, Jingchang Chen, Jingyang Yuan, Junjie Qiu, Junlong Li, J. L. Cai, Jiaqi Ni, Jian Liang, Jin Chen, Kai Dong, Kai Hu, Kaige Gao, Kang Guan, Kexin Huang, Kuai Yu, Lean Wang, Lecong Zhang, Liang Zhao, Litong Wang, Liyue Zhang, Lei Xu, Leyi Xia, Mingchuan Zhang, Minghua Zhang, Minghui Tang, Meng Li, Miaojun Wang, Mingming Li, Ning Tian, Panpan Huang, Peng Zhang, Qiancheng Wang, Qinyu Chen, Qiushi Du, Ruiqi Ge, Ruisong Zhang, Ruizhe Pan, Runji Wang, R. J. Chen, R. L. Jin, Ruyi Chen, Shanghao Lu, Shangyan Zhou, Shanhuang Chen, Shengfeng Ye, Shiyu Wang, Shuiping Yu, Shunfeng Zhou, Shuting Pan, S. S. Li, Shuang Zhou, Shaoqing Wu, Shengfeng Ye, Tao Yun, Tian Pei, Tianyu Sun, T. Wang, Wangding Zeng, Wanbiao Zhao, Wen Liu, Wenfeng Liang, Wenjun Gao, Wenqin Yu, Wentao Zhang, W. L. Xiao, Wei An, Xiaodong Liu, Xiaohan Wang, Xiaokang Chen, Xiaotao Nie, Xin Cheng, Xin Liu, Xin Xie, Xingchao Liu, Xinyu Yang, Xinyuan Li, Xuecheng Su, Xuheng Lin, X. Q. Li, Xiangyue Jin, Xiaojin Shen, Xiaosha Chen, Xiaowen Sun, Xiaoxiang Wang, Xinnan Song, Xinyi Zhou, Xianzu Wang, Xinxia Shan, Y. K. Li, Y. Q. Wang, Y. X. Wei, Yang Zhang, Yanhong Xu, Yao Li, Yao Zhao, Yaofeng Sun, Yaohui Wang, Yi Yu, Yichao Zhang, Yifan Shi, Yiliang Xiong, Ying He, Yishi Piao, Yisong Wang, Yixuan Tan, Yiyang Ma, Yiyuan Liu, Yongqiang Guo, Yuan Ou, Yuduan Wang, Yue Gong, Yuheng Zou, Yujia He, Yunfan Xiong, Yuxiang Luo, Yuxiang You, Yuxuan Liu, Yuyang Zhou, Y. X. Zhu, Yanhong Xu, Yanping Huang, Yaohui Li, Yi Zheng, Yuchen Zhu, Yunxian Ma, Ying Tang, Yukun Zha, Yuting Yan, Z. Z. Ren, Zehui Ren, Zhangli Sha, Zhe Fu, Zhean Xu, Zhenda Xie, Zhengyan Zhang, Zhewen Hao, Zhicheng Ma, Zhigang Yan, Zhiyu Wu, Zihui Gu, Zijia Zhu, Zijun Liu, Zilin Li, Ziwei Xie, Ziyang Song, Zizheng Pan, Zhen Huang, Zhipeng Xu, Zhongyu Zhang, and Zhen Zhang. Deepseek-r1: Incentivizing reasoning capability in llms via reinforcement learning, 2025. URL <https://arxiv.org/abs/2501.12948>.
- [2] Aaron Jaech, Adam Kalai, Adam Lerer, Adam Richardson, Ahmed El-Kishky, Aiden Low, Alec Helyar, Aleksander Madry, Alex Beutel, Alex Carney, Alex Iftimie, Alex Karpenko, Alex Tachard Passos, Alexander Neitz, Alexander Prokofiev, Alexander Wei, Allison Tam, Ally Bennett, Ananya Kumar, Andre Saraiva, Andrea Vallone, Andrew Duberstein, Andrew Kondrich, Andrey Mishchenko, Andy Applebaum, Angela Jiang, Ashvin Nair, Barret Zoph, Behrooz Ghorbani, Ben Rossen, Benjamin Sokolowsky, Boaz Barak, Bob McGrew, Borys Minaiev, Botao Hao, Bowen Baker, Brandon Houghton, Brandon McKinzie, Brydon Eastman, Camillo Lugaresi, Cary Bassin, Cary Hudson, Chak Ming Li, Charles de Bourcy, Chelsea Voss, Chen Shen, Chong Zhang, Chris Koch, Chris Orsinger, Christopher Hesse, Claudia Fischer, Clive Chan, Dan Roberts, Daniel Kappler, Daniel Levy, Daniel Selsam, David Dohan, David Farhi, David Mely, David Robinson, Dimitris Tsipras, Doug Li, Dragos Oprica, Eben Freeman, Eddie Zhang, Edmund Wong, Elizabeth Proehl, Enoch Cheung, Eric Mitchell, Eric Wallace, Erik Ritter, Evan Mays, Fan Wang, Felipe Petroski Such, Filippo Raso, Florencia Leoni, Foivos Tsimpourlas, Francis Song, Fred von Lohmann, Freddie Sulit, Geoff Salmon, Giambattista Parascandolo, Gildas Chabot, Grace Zhao, Greg Brockman, Guillaume Leclerc, Hadi Salman, Haiming Bao, Hao Sheng, Hart Andrin, Hessam Bagherinezhad, Hongyu Ren, Hunter Lightman, Hyung Won Chung, Ian Kivlichan, Ian O’Connell, Ian Osband, Ignasi Clavera Gilaberte, and Ilge Akkaya. Openai o1

- system card. *arXiv*, 2412.16720, 2024. URL <https://doi.org/10.48550/arXiv.2412.16720>.
- [3] Niklas Muennighoff, Zitong Yang, Weijia Shi, Xiang Lisa Li, Li Fei-Fei, Hannaneh Hajishirzi, Luke Zettlemoyer, Percy Liang, Emmanuel Candès, and Tatsunori Hashimoto. s1: Simple test-time scaling, 2025. URL <https://arxiv.org/abs/2501.19393>.
- [4] Bowen Jin, Hansi Zeng, Zhenrui Yue, Dong Wang, Hamed Zamani, and Jiawei Han. Search-r1: Training llms to reason and leverage search engines with reinforcement learning. *arXiv*, 2503.09516, 2025. URL <https://doi.org/10.48550/arXiv.2503.09516>.
- [5] Xiaoxi Li, Guanting Dong, Jiajie Jin, Yuyao Zhang, Yujia Zhou, Yutao Zhu, Peitian Zhang, and Zhicheng Dou. Search-o1: Agentic search-enhanced large reasoning models. *arXiv*, 2501.05366, 2025. URL <https://doi.org/10.48550/arXiv.2501.05366>.
- [6] Wenhui Chen, Xueguang Ma, Xinyi Wang, and William W. Cohen. Program of thoughts prompting: Disentangling computation from reasoning for numerical reasoning tasks. *Trans. Mach. Learn. Res.*, 2023, 2023. URL <https://openreview.net/forum?id=YfZ4ZPt8zd>.
- [7] Xin Lai, Junyi Li, Wei Li, Tao Liu, Tianjian Li, and Hengshuang Zhao. Mini-o3: Scaling up reasoning patterns and interaction turns for visual search. *arXiv*, 2509.07969, 2025. URL <https://doi.org/10.48550/arXiv.2509.07969>.
- [8] Penghao Wu and Saining Xie. V*: Guided visual search as a core mechanism in multimodal llms. In *IEEE/CVF Conference on Computer Vision and Pattern Recognition, CVPR 2024, Seattle, WA, USA, June 16-22, 2024*, pages 13084–13094. IEEE, 2024. URL <https://doi.org/10.1109/CVPR52733.2024.01243>.
- [9] Junde Wu, Jiayuan Zhu, and Yuyuan Liu. Agentic reasoning: Reasoning llms with tools for the deep research. *arXiv*, 2502.04644, 2025. URL <https://doi.org/10.48550/arXiv.2502.04644>.
- [10] Zhibin Gou, Zhihong Shao, Yeyun Gong, Yelong Shen, Yujiu Yang, Minlie Huang, Nan Duan, and Weizhu Chen. Tora: A tool-integrated reasoning agent for mathematical problem solving. In *The Twelfth International Conference on Learning Representations, ICLR 2024, Vienna, Austria, May 7-11, 2024*. OpenReview.net, 2024. URL <https://openreview.net/forum?id=Ep0TtjVoap>.
- [11] Heng Lin and Zhongwen Xu. Understanding tool-integrated reasoning. *arXiv*, 2508.19201, 2025. URL <https://doi.org/10.48550/arXiv.2508.19201>.
- [12] Shitian Zhao, Haoquan Zhang, Shaoheng Lin, Ming Li, Qilong Wu, Kaipeng Zhang, and Chen Wei. Pyvision: Agentic vision with dynamic tooling. *arXiv*, 2507.07998, 2025. URL <https://doi.org/10.48550/arXiv.2507.07998>.
- [13] Hongjin Su, Shizhe Diao, Ximing Lu, Mingjie Liu, Jiacheng Xu, Xin Dong, Yonggan Fu, Peter Belcak, Hanrong Ye, Hongxu Yin, Yi Dong, Evelina Bakhturina, Tao Yu, Yejin Choi, Jan Kautz, and Pavlo Molchanov. Toolorchestra: Elevating intelligence via efficient model and tool orchestration. *arXiv*, 2511.21689, 2025. URL <https://doi.org/10.48550/arXiv.2511.21689>.
- [14] Yushi Hu, Weijia Shi, Xingyu Fu, Dan Roth, Mari Ostendorf, Luke Zettlemoyer, Noah A. Smith, and Ranjay Krishna. Visual sketchpad: Sketching as a visual chain of thought for multimodal language models. In *The Thirty-eighth Annual Conference on Neural Information Processing Systems*, 2024. URL <https://openreview.net/forum?id=GNSM11P5VR>.

-
- [15] Sara Vera Marjanovic, Arkil Patel, Vaibhav Adlakha, Milad Aghajohari, Parishad BehnamGhader, Mehar Bhatia, Aditi Khandelwal, Austin Kraft, Benno Krojer, Xing Han Lù, Nicholas Meade, Dongchan Shin, Amirhossein Kazemnejad, Gaurav Kamath, Marius Mosbach, Karolina Stanczak, and Siva Reddy. Deepseek-r1 thoughtology: Let’s think about LLM reasoning. *Trans. Mach. Learn. Res.*, 2026, 2026. URL <https://openreview.net/forum?id=BZwKsiRnJI>.
- [16] Shu Yang, Junchao Wu, Xin Chen, Yunze Xiao, Xinyi Yang, Derek F. Wong, and Di Wang. Understanding aha moments: from external observations to internal mechanisms, 2025. URL <https://arxiv.org/abs/2504.02956>.
- [17] Jeonghye Kim, Xufang Luo, Minbeom Kim, Sangmook Lee, Dongsheng Li, and Yuqing Yang. Understanding reasoning in llms through strategic information allocation under uncertainty, 2026. URL <https://arxiv.org/abs/2603.15500>.
- [18] Shitian Zhao, Shaoheng Lin, Ming Li, Haoquan Zhang, Wenshuo Peng, Kaipeng Zhang, and Chen Wei. Pyvision-rl: Forging open agentic vision models via RL. *arXiv*, 2602.20739, 2026. URL <https://doi.org/10.48550/arXiv.2602.20739>.
- [19] Qwen Team. Qwen3-vl technical report. *arXiv*, 2511.21631, 2025. URL <https://doi.org/10.48550/arXiv.2511.21631>.
- [20] Minki Kang, Jongwon Jeong, Seanie Lee, Jaewoong Cho, and Sung Ju Hwang. Distilling LLM agent into small models with retrieval and code tools. In *The Thirty-ninth Annual Conference on Neural Information Processing Systems*, 2025. URL <https://openreview.net/forum?id=VkiCTqsZ0n>.
- [21] Stéphane Ross, Geoffrey J. Gordon, and Drew Bagnell. A reduction of imitation learning and structured prediction to no-regret online learning. In Geoffrey J. Gordon, David B. Dunson, and Miroslav Dudík, editors, *Proceedings of the Fourteenth International Conference on Artificial Intelligence and Statistics, AISTATS 2011, Fort Lauderdale, USA, April 11-13, 2011*, JMLR Proceedings, pages 627–635. JMLR.org, 2011. URL <http://proceedings.mlr.press/v15/ross11a/ross11a.pdf>.
- [22] Joykirat Singh, Raghav Magazine, Yash Pandya, and Akshay Nambi. Agentic reasoning and tool integration for llms via reinforcement learning, 2025. URL <https://arxiv.org/abs/2505.01441>.
- [23] Jack Hong, Chenxiao Zhao, ChengLin Zhu, Weiheng Lu, Guohai Xu, and Xing Yu. Deepeyesv2: Toward agentic multimodal model, 2025. URL <https://arxiv.org/abs/2511.05271>.
- [24] Zhihong Shao, Peiyi Wang, Qihao Zhu, Runxin Xu, Junxiao Song, Mingchuan Zhang, Y. K. Li, Y. Wu, and Daya Guo. Deepseekmath: Pushing the limits of mathematical reasoning in open language models. *arXiv*, 2402.03300, 2024. URL <https://doi.org/10.48550/arXiv.2402.03300>.
- [25] Qiying Yu, Zheng Zhang, Ruofei Zhu, Yufeng Yuan, Xiaochen Zuo, Yu Yue, Tiantian Fan, Gaohong Liu, Lingjun Liu, Xin Liu, Haibin Lin, Zhiqi Lin, Bole Ma, Guangming Sheng, Yuxuan Tong, Chi Zhang, Mofan Zhang, Wang Zhang, Hang Zhu, Jinhua Zhu, Jiase Chen, Jiangjie Chen, Chengyi Wang, Honglin Yu, Weinan Dai, Yuxuan Song, Xiang Wei, Haodong Zhou, Jingjing Liu, Wei Ma, Ya-Qin Zhang, Lin Yan, Mu Qiao, Yong-Xu Wu, and Mingxuan Wang. Dapo: An open-source llm reinforcement learning system at scale. *arXiv*, 2503.14476, 2025. URL <https://api.semanticscholar.org/CorpusID:277104124>.
-

-
- [26] Mingjie Liu, Shizhe Diao, Ximing Lu, Jian Hu, Xin Dong, Yejin Choi, Jan Kautz, and Yi Dong. ProRL: Prolonged reinforcement learning expands reasoning boundaries in large language models. In *The Thirty-ninth Annual Conference on Neural Information Processing Systems*, 2026. URL <https://openreview.net/forum?id=YPsJha5HXQ>.
- [27] Yuxiao Qu, Amrith Setlur, Virginia Smith, Ruslan Salakhutdinov, and Aviral Kumar. POPE: learning to reason on hard problems via privileged on-policy exploration. *arXiv*, 2601.18779, 2026. URL <https://doi.org/10.48550/arXiv.2601.18779>.
- [28] Baohao Liao, Hanze Dong, Xinxing Xu, Christof Monz, and Jiang Bian. Self-hinting language models enhance reinforcement learning. *arXiv*, 2602.03143, 2026. URL <https://doi.org/10.48550/arXiv.2602.03143>.
- [29] Hongru Wang, Cheng Qian, Wanjun Zhong, Xiusi Chen, Jiahao Qiu, Shijue Huang, Bowen Jin, Mengdi Wang, Kam-Fai Wong, and Heng Ji. Acting less is reasoning more! teaching model to act efficiently, 2025. URL <https://arxiv.org/abs/2504.14870>.
- [30] Jian Hu, Mingjie Liu, Ximing Lu, Fang Wu, Zaïd Harchaoui, Shizhe Diao, Yejin Choi, Pavlo Molchanov, June Yang, Jan Kautz, and Yi Dong. Brorl: Scaling reinforcement learning via broadened exploration. *arXiv*, 2510.01180, 2025. URL <https://doi.org/10.48550/arXiv.2510.01180>.
- [31] Guanting Dong, Hangyu Mao, Kai Ma, Licheng Bao, Yifei Chen, Zhongyuan Wang, Zhongxia Chen, Jiazhen Du, Huiyang Wang, Fuzheng Zhang, Guorui Zhou, Yutao Zhu, Ji-Rong Wen, and Zhicheng Dou. Agentic reinforced policy optimization. In *The Fourteenth International Conference on Learning Representations*, 2026. URL <https://openreview.net/forum?id=TX4k7BF6a0>.
- [32] John Schulman, Filip Wolski, Prafulla Dhariwal, Alec Radford, and Oleg Klimov. Proximal policy optimization algorithms. *arXiv*, 1707.06347, 2017. URL <http://arxiv.org/abs/1707.06347>.
- [33] Zihan Wang, Chi Gui, Xing Jin, Qineng Wang, Licheng Liu, Kangrui Wang, Shiqi Chen, Linjie Li, Zhengyuan Yang, Pingyue Zhang, Yiping Lu, Jiajun Wu, Li Fei-Fei, Lijuan Wang, Yejin Choi, and Manling Li. Ragen-2: Reasoning collapse in agentic rl, 2026. URL <https://arxiv.org/abs/2604.06268>.
- [34] Yichao Fu, Xuewei Wang, Yuandong Tian, and Jiawei Zhao. Deep think with confidence. *arXiv*, 2025. URL <https://arxiv.org/abs/2508.15260>.
- [35] Haozhe Wang, Chao Qu, Zuming Huang, Wei Chu, Fangzhen Lin, and Wenhui Chen. V1-rethinker: Incentivizing self-reflection of vision-language models with reinforcement learning. *arXiv*, 2504.08837, 2025. URL <https://doi.org/10.48550/arXiv.2504.08837>.
- [36] Jinming Wu, Zihao Deng, Wei Li, Yiding Liu, Bo You, Bo Li, Zejun Ma, and Ziwei Liu. Mmsearch-rl: Incentivizing llms to search. 2025. URL <https://arxiv.org/abs/2506.20670>.
- [37] Honglin Lin, Zheng Liu, Yun Zhu, Chonghan Qin, Juekai Lin, Xiaoran Shang, Conghui He, Wentao Zhang, and Lijun Wu. Mmfinereason: Closing the multimodal reasoning gap via open data-centric methods. *arXiv*, 2601.21821, 2026. URL <https://doi.org/10.48550/arXiv.2601.21821>.
- [38] Ke Wang, Junting Pan, Weikang Shi, Zimu Lu, Mingjie Zhan, and Hongsheng Li. Measuring multimodal mathematical reasoning with math-vision dataset. *arXiv*, 2024. URL <https://arxiv.org/abs/2402.14804>.
-

-
- [39] Chengke Zou, Xingang Guo, Rui Yang, Junyu Zhang, Bin Hu, and Huan Zhang. Dynamath: A dynamic visual benchmark for evaluating mathematical reasoning robustness of vision language models. In *The Thirteenth International Conference on Learning Representations, ICLR 2025, Singapore, April 24-28, 2025*. OpenReview.net, 2025. URL <https://openreview.net/forum?id=VOAMTA8jKu>.
- [40] Chengqi Duan, Kaiyue Sun, Rongyao Fang, Manyuan Zhang, Yan Feng, Ying Luo, Yufang Liu, Ke Wang, Peng Pei, Xunliang Cai, Hongsheng Li, Yi Ma, and Xihui Liu. Codeplotcot: Mathematical visual reasoning by thinking with code-driven images, 2025. URL <https://arxiv.org/abs/2510.11718>.
- [41] Wenbin Wang, Liang Ding, Minyan Zeng, Xiabin Zhou, Li Shen, Yong Luo, Wei Yu, and Dacheng Tao. Divide, conquer and combine: A training-free framework for high-resolution image perception in multimodal large language models. In Toby Walsh, Julie Shah, and Zico Kolter, editors, *Thirty-Ninth AAAI Conference on Artificial Intelligence, Thirty-Seventh Conference on Innovative Applications of Artificial Intelligence, Fifteenth Symposium on Educational Advances in Artificial Intelligence, AAAI 2025, Philadelphia, PA, USA, February 25 - March 4, 2025*, pages 7907–7915. AAAI Press, 2025. URL <https://doi.org/10.1609/aaai.v39i8.32852>.
- [42] Yong Xien Chng, Tao Hu, Wenwen Tong, Xueheng Li, Jiandong Chen, Haojia Yu, Jiefan Lu, Hwei Guo, Hanming Deng, Xie Chen, Gao Huang, Dahua Lin, and Lewei Lu. Sensenovamars: Empowering multimodal agentic reasoning and search via reinforcement learning. *arXiv*, 2512.24330, 2025. URL <https://doi.org/10.48550/arXiv.2512.24330>.
- [43] Dongzhi Jiang, Renrui Zhang, Ziyu Guo, Yanmin Wu, Jiayi Lei, Pengshuo Qiu, Pan Lu, Zehui Chen, Guanglu Song, Peng Gao, Yu Liu, Chunyuan Li, and Hongsheng Li. Mmsearch: Benchmarking the potential of large models as multi-modal search engines. *arXiv*, 2409.12959, 2024. URL <https://doi.org/10.48550/arXiv.2409.12959>.
- [44] Alex Su, Haozhe Wang, Weiming Ren, Fangzhen Lin, and Wenhui Chen. Pixel reasoner: Incentivizing pixel space reasoning via curiosity-driven reinforcement learning. In *The Thirty-ninth Annual Conference on Neural Information Processing Systems*, 2026. URL <https://openreview.net/forum?id=VeZkY3JjWV>.
- [45] Ziwei Zheng, Michael Yang, Jack Hong, Chenxiao Zhao, Guohai Xu, Le Yang, Chao Shen, and XingYu. Deepeyes: Incentivizing "thinking with images" via reinforcement learning. In *The Fourteenth International Conference on Learning Representations*, 2026. URL <https://openreview.net/forum?id=xUyMXkI958>.
- [46] Yuda Song, Lili Chen, Fahim Tajwar, Remi Munos, Deepak Pathak, J. Andrew Bagnell, Aarti Singh, and Andrea Zanette. Expanding the capabilities of reinforcement learning via text feedback, 2026. URL <https://arxiv.org/abs/2602.02482>.
- [47] MiniMax, :, Aili Chen, Aonian Li, Bangwei Gong, Binyang Jiang, Bo Fei, Bo Yang, Boji Shan, Changqing Yu, Chao Wang, Cheng Zhu, Chengjun Xiao, Chengyu Du, Chi Zhang, Chu Qiao, Chunhao Zhang, Chunhui Du, Congchao Guo, Da Chen, Deming Ding, Dianjun Sun, Dong Li, Enwei Jiao, Haigang Zhou, Haimo Zhang, Han Ding, Haohai Sun, Haoyu Feng, Huaiguang Cai, Haichao Zhu, Jian Sun, Jiaqi Zhuang, Jiaren Cai, Jiayuan Song, Jin Zhu, Jingyang Li, Jinhao Tian, Jinli Liu, Junhao Xu, Junjie Yan, Junteng Liu, Junxian He, Kaiyi Feng, Ke Yang, Kecheng Xiao, Le Han, Leyang Wang, Lianfei Yu, Liheng Feng, Lin Li, Lin Zheng, Linge Du, Lingyu Yang, Lunbin Zeng, Minghui Yu, Mingliang Tao, Mingyuan Chi, Mozhi Zhang, Mujie Lin, Nan Hu, Nongyu Di, Peng Gao, Pengfei Li, Pengyu Zhao, Qibing Ren, Qidi Xu, Qile Li,
-

- Qin Wang, Rong Tian, Ruitao Leng, Shaoxiang Chen, Shaoyu Chen, Shengmin Shi, Shitong Weng, Shuchang Guan, Shuqi Yu, Sichen Li, Songquan Zhu, Tengfei Li, Tianchi Cai, Tianrun Liang, Weiyu Cheng, Weize Kong, Wenkai Li, Xiancai Chen, Xiangjun Song, Xiao Luo, Xiao Su, Xiaobo Li, Xiaodong Han, Xinzhu Hou, Xuan Lu, Xun Zou, Xuyang Shen, Yan Gong, Yan Ma, Yang Wang, Yiqi Shi, Yiran Zhong, Yonghong Duan, Yongxiang Fu, Yongyi Hu, Yu Gao, Yuanxiang Fan, Yufeng Yang, Yuhao Li, Yulin Hu, Yunan Huang, Yunji Li, Yunzhi Xu, Yuxin Mao, Yuxuan Shi, Yuze Wenren, Zehan Li, Zelin Li, Zhanxu Tian, Zhengmao Zhu, Zhenhua Fan, Zhenzhen Wu, Zhichao Xu, Zhihang Yu, Zhiheng Lyu, Zhuo Jiang, Zibo Gao, Zijia Wu, Zijian Song, and Zijun Sun. Minimax-m1: Scaling test-time compute efficiently with lightning attention, 2025. URL <https://arxiv.org/abs/2506.13585>.
- [48] Shunyu Yao, Jeffrey Zhao, Dian Yu, Nan Du, Izhak Shafran, Karthik R. Narasimhan, and Yuan Cao. React: Synergizing reasoning and acting in language models. In *The Eleventh International Conference on Learning Representations, ICLR 2023, Kigali, Rwanda, May 1-5, 2023*. OpenReview.net, 2023. URL https://openreview.net/forum?id=WE_vluYUL-X.
- [49] Jiazhan Feng, Shijue Huang, Xingwei Qu, Ge Zhang, Yujia Qin, Baoquan Zhong, Chengquan Jiang, Jinxin Chi, and Wanjun Zhong. Retool: Reinforcement learning for strategic tool use in llms. *arXiv*, 2504.11536, 2025. URL <https://arxiv.org/abs/2504.11536>.
- [50] Ke Wang, Houxing Ren, Aojun Zhou, Zimu Lu, Sichun Luo, Weikang Shi, Renrui Zhang, Linqi Song, Mingjie Zhan, and Hongsheng Li. Mathcoder: Seamless code integration in llms for enhanced mathematical reasoning. *arXiv*, 2310.03731, 2023. URL <https://arxiv.org/abs/2310.03731>.
- [51] Minki Kang, Jongwon Jeong, and Jaewoong Cho. T1: Tool-integrated verification for test-time compute scaling in small language models. In *The Fourteenth International Conference on Learning Representations*, 2026. URL <https://openreview.net/forum?id=tBkLWfmugI>.
- [52] Google Deepmind. Introducing agentic vision in gemini 3 flash. <https://blog.google/innovation-and-ai/technology/developers-tools/agentic-vision-gemini-3-flash/>, 2025.
- [53] OpenAI. Thinking with images. <https://openai.com/index/thinking-with-images/>, 2025.
- [54] Runqi Qiao, Qiuna Tan, Minghan Yang, Guanting Dong, Peiqing Yang, Shiqiang Lang, Enhui Wan, Xiaowan Wang, Yida Xu, Lan Yang, Chong Sun, Chen Li, Jing Lyu, and Honggang Zhang. V-thinker: Interactive thinking with images, 2025. URL <https://arxiv.org/abs/2511.04460>.
- [55] Ning Shang, Yifei Liu, Yi Zhu, Li Lyna Zhang, Weijiang Xu, Xinyu Guan, Buze Zhang, Bingcheng Dong, Xudong Zhou, Bowen Zhang, Ying Xin, Ziming Miao, Scarlett Li, Fan Yang, and Mao Yang. rstar2-agent: Agentic reasoning technical report. *arXiv*, 2508.20722, 2025. URL <https://doi.org/10.48550/arXiv.2508.20722>.
- [56] Cheng Qian, Emre Can Acikgoz, Qi He, Hongru Wang, Xiusi Chen, Dilek Hakkani-Tür, Gokhan Tur, and Heng Ji. Toolrl: Reward is all tool learning needs, 2025. URL <https://arxiv.org/abs/2504.13958>.
- [57] Xuefeng Li, Haoyang Zou, and Pengfei Liu. Torl: Scaling tool-integrated RL. *arXiv*, 2503.23383, 2025. URL <https://doi.org/10.48550/arXiv.2503.23383>.
- [58] Yifan Zhang, Xingyu Lu, Shukang Yin, Chaoyou Fu, Wei Chen, Xiao Hu, Bin Wen, Kaiyu Jiang, Changyi Liu, Tianke Zhang, Haonan Fan, Kaibing Chen, Jiankang Chen, Haojie Ding,

- Kaiyu Tang, Zhang Zhang, Liang Wang, Fan Yang, Tingting Gao, and Guorui Zhou. Thyme: Think beyond images. *arXiv*, 2508.11630, 2025. URL <https://doi.org/10.48550/arXiv.2508.11630>.
- [59] Guanting Dong, Licheng Bao, Zhongyuan Wang, Kangzhi Zhao, Xiaoxi Li, Jiajie Jin, Jinghan Yang, Hangyu Mao, Fuzheng Zhang, Kun Gai, Guorui Zhou, Yutao Zhu, Ji-Rong Wen, and Zhicheng Dou. Agentic entropy-balanced policy optimization. *arXiv*, 2025. URL <https://arxiv.org/abs/2510.14545>.
- [60] Guangming Sheng, Chi Zhang, Zilingfeng Ye, Xibin Wu, Wang Zhang, Ru Zhang, Yanghua Peng, Haibin Lin, and Chuan Wu. Hybridflow: A flexible and efficient rlhf framework. *arXiv preprint arXiv: 2409.19256*, 2024.
- [61] Sijun Tan, Michael Luo, Colin Cai, Tarun Venkat, Kyle Montgomery, Aaron Hao, Tianhao Wu, Arnav Balyan, Manan Roongta, Chenguang Wang, Li Erran Li, Raluca Ada Popa, and Ion Stoica. rllm: A framework for post-training language agents. <https://pretty-radio-b75.notion.site/rLLM-A-Framework-for-Post-Training-Language-Agents\ -21b81902c146819db63cd98a54ba5f31>, 2025. Notion Blog.
- [62] Yang Yue, Zhiqi Chen, Rui Lu, Andrew Zhao, Zhaokai Wang, Yang Yue, Shiji Song, and Gao Huang. Does reinforcement learning really incentivize reasoning capacity in LLMs beyond the base model? In *The Thirty-ninth Annual Conference on Neural Information Processing Systems*, 2026. URL <https://openreview.net/forum?id=40sgYD7em5>.
- [63] Tianzhe Chu, Yuexiang Zhai, Jihan Yang, Shengbang Tong, Saining Xie, Dale Schuurmans, Quoc V. Le, Sergey Levine, and Yi Ma. Sft memorizes, rl generalizes: A comparative study of foundation model post-training, 2025. URL <https://arxiv.org/abs/2501.17161>.
- [64] Shuai Bai, Keqin Chen, Xuejing Liu, Jialin Wang, Wenbin Ge, Sibao Song, Kai Dang, Peng Wang, Shijie Wang, Jun Tang, Humen Zhong, Yuanzhi Zhu, Ming-Hsuan Yang, Zhaohai Li, Jianqiang Wan, Pengfei Wang, Wei Ding, Zheren Fu, Yiheng Xu, Jiabo Ye, Xi Zhang, Tianbao Xie, Zesen Cheng, Hang Zhang, Zhibo Yang, Haiyang Xu, and Junyang Lin. Qwen2.5-vl technical report. *arXiv*, 2502.13923, 2025. URL <https://doi.org/10.48550/arXiv.2502.13923>.
- [65] Woosuk Kwon, Zhuohan Li, Siyuan Zhuang, Ying Sheng, Lianmin Zheng, Cody Hao Yu, Joseph E. Gonzalez, Hao Zhang, and Ion Stoica. Efficient memory management for large language model serving with pagedattention. In *Proceedings of the ACM SIGOPS 29th Symposium on Operating Systems Principles*, 2023.
- [66] Baian Chen, Chang Shu, Ehsan Shareghi, Nigel Collier, Karthik Narasimhan, and Shunyu Yao. Fireact: Toward language agent fine-tuning. *arXiv*, 2310.05915, 2023. URL <https://doi.org/10.48550/arXiv.2310.05915>.
- [67] Byung-Kwan Lee, Ryo Hachiuma, Yong Man Ro, Frank Wang, and Yueh-Hua Wu. Unified reinforcement and imitation learning for vision-language models. In D. Belgrave, C. Zhang, H. Lin, R. Pascanu, P. Koniusz, M. Ghassemi, and N. Chen, editors, *Advances in Neural Information Processing Systems*, volume 38, pages 156508–156534. Curran Associates, Inc., 2025. URL https://proceedings.neurips.cc/paper_files/paper/2025/file/e58497367bc8730f61a87d37800c0a06-Paper-Conference.pdf.
- [68] Byung-Kwan Lee, Yu-Chiang Frank Wang, and Ryo Hachiuma. Masking teacher and reinforcing student for distilling vision-language models, 2025. URL <https://arxiv.org/abs/2512.22238>.

-
- [69] Jiwan Kim, Kibum Kim, Wonjoong Kim, Byung-Kwan Lee, and Chanyoung Park. Why and when visual token pruning fails? a study on relevant visual information shift in mllms decoding, 2026. URL <https://arxiv.org/abs/2604.12358>.
- [70] Seonghoon Yu, Dongjun Nam, Byung-Kwan Lee, and Jeany Son. Hide to see: Reasoning-prefix masking for visual-anchored thinking in vlm distillation, 2026. URL <https://arxiv.org/abs/2605.11651>.
- [71] Byung-Kwan Lee, Ryo Hachiuma, Yong Man Ro, Yu-Chiang Frank Wang, and Yueh-Hua Wu. Genrecal: Generation after recalibration from large to small vision-language models, 2026. URL <https://arxiv.org/abs/2506.15681>.
- [72] Byung-Kwan Lee, Ryo Hachiuma, Yu-Chiang Frank Wang, Yong Man Ro, and Yueh-Hua Wu. Vlsi: Verbalized layers-to-interactions from large to small vision language models. In *Proceedings of the IEEE/CVF Conference on Computer Vision and Pattern Recognition (CVPR)*, pages 29545–29557, June 2025.
- [73] Young-Jun Lee, Seungone Kim, Byung-Kwan Lee, Minkyong Moon, Yechan Hwang, Jong Myoung Kim, Graham Neubig, Sean Welleck, and Ho-Jin Choi. Refinebench: Evaluating refinement capability of language models via checklists, 2025. URL <https://arxiv.org/abs/2511.22173>.
- [74] Young-Jun Lee, Byung-Kwan Lee, Jianshu Zhang, Yechan Hwang, Byungsoo Ko, Han-Gyu Kim, Dongyu Yao, Xuankun Rong, Eojin Joo, Seung-Ho Han, Bowon Ko, and Ho-Jin Choi. Multiverse: A multi-turn conversation benchmark for evaluating large vision and language models. In *Proceedings of the IEEE/CVF International Conference on Computer Vision (ICCV)*, pages 708–719, October 2025.
- [75] Youngjoon Yu, Sangyun Chung, Byung-Kwan Lee, and Yong Man Ro. Spark: Multi-vision sensor perception and reasoning benchmark for large-scale vision-language models, 2024. URL <https://arxiv.org/abs/2408.12114>.
- [76] Byung-Kwan Lee, Chae Won Kim, Beomchan Park, and Yong Man Ro. Meteor: Mamba-based traversal of rationale for large language and vision models. In A. Globerson, L. Mackey, D. Belgrave, A. Fan, U. Paquet, J. Tomczak, and C. Zhang, editors, *Advances in Neural Information Processing Systems*, volume 37, pages 40278–40315. Curran Associates, Inc., 2024. doi: 10.52202/079017-1274. URL https://proceedings.neurips.cc/paper_files/paper/2024/file/473a9a75edc46eff5ff224d53d5f7294-Paper-Conference.pdf.
- [77] Byung-Kwan Lee, Beomchan Park, Chae Won Kim, and Yong Man Ro. Moai: Mixture of all intelligence for large language and vision models. In Aleš Leonardis, Elisa Ricci, Stefan Roth, Olga Russakovsky, Torsten Sattler, and Gül Varol, editors, *Computer Vision – ECCV 2024*, pages 273–302, Cham, 2025. Springer Nature Switzerland. ISBN 978-3-031-72967-6.
- [78] Byung-Kwan Lee, Beomchan Park, Chae Won Kim, and Yong Man Ro. CoLLaVO: Crayon large language and vision mOdel. In Lun-Wei Ku, Andre Martins, and Vivek Srikumar, editors, *Findings of the Association for Computational Linguistics: ACL 2024*, pages 1121–1138, Bangkok, Thailand, August 2024. Association for Computational Linguistics. doi: 10.18653/v1/2024.findings-acl.66. URL <https://aclanthology.org/2024.findings-acl.66/>.
- [79] Byung-Kwan Lee, Sangyun Chung, Chae Won Kim, Beomchan Park, and Yong Man Ro. Phantom of latent for large language and vision models, 2024. URL <https://arxiv.org/abs/2409.14713>.
-

- [80] Qwen Team. Qwen3.5: Accelerating productivity with native multimodal agents, February 2026. URL <https://qwen.ai/blog?id=qwen3.5>.
- [81] Junho Kim, Byung-Kwan Lee, and Yong Man Ro. Distilling robust and non-robust features in adversarial examples by information bottleneck. In M. Ranzato, A. Beygelzimer, Y. Dauphin, P.S. Liang, and J. Wortman Vaughan, editors, *Advances in Neural Information Processing Systems*, volume 34, pages 17148–17159. Curran Associates, Inc., 2021. URL https://proceedings.neurips.cc/paper_files/paper/2021/file/8e5e15c4e6d09c8333a17843461041a9-Paper.pdf.
- [82] Byung-Kwan Lee, Junho Kim, and Yong Man Ro. Masking adversarial damage: Finding adversarial saliency for robust and sparse network. In *Proceedings of the IEEE/CVF Conference on Computer Vision and Pattern Recognition (CVPR)*, pages 15126–15136, June 2022.
- [83] Junho Kim, Byung-Kwan Lee, and Yong Man Ro. Demystifying causal features on adversarial examples and causal inoculation for robust network by adversarial instrumental variable regression. In *Proceedings of the IEEE/CVF Conference on Computer Vision and Pattern Recognition (CVPR)*, pages 12302–12312, June 2023.
- [84] Byung-Kwan Lee, Junho Kim, and Yong Man Ro. Mitigating adversarial vulnerability through causal parameter estimation by adversarial double machine learning. In *Proceedings of the IEEE/CVF International Conference on Computer Vision (ICCV)*, pages 4499–4509, October 2023.
- [85] Byung-Kwan Lee, Youngjoon Yu, and Yong Man Ro. Towards adversarial robustness of bayesian neural network through hierarchical variational inference, 2021. URL <https://openreview.net/forum?id=Cue2ZEBf12>.
- [86] Yeonju Kim, Junho Kim, Byung-Kwan Lee, Sebin Shin, and Yong Man Ro. Mitigating dataset bias in image captioning through clip confounder-free captioning network. In *2023 IEEE International Conference on Image Processing (ICIP)*, pages 1720–1724, 2023. doi: 10.1109/ICIP49359.2023.10222502.
- [87] Junho Kim, Byung-Kwan Lee, and Yong Man Ro. Causal unsupervised semantic segmentation. *Pattern Recognition*, 171:112173, 2026. ISSN 0031-3203. doi: <https://doi.org/10.1016/j.patcog.2025.112173>. URL <https://www.sciencedirect.com/science/article/pii/S0031320325008349>.

A. Experimental Setup

This section expands on [Section 4.1](#): training data and hyperparameters ([Appendix A.1](#)), the agentic system prompt and tool schemas ([Appendix A.2](#)), and per-benchmark descriptions ([Appendix A.3](#)).

A.1. Training

We expand on [Section 4.1](#) with the full training data composition and hyperparameter list.

SFT data composition. SFT uses 64,274 trajectories drawn from three sources: ViRL [35], fvqa [36], and PyVision-RL [18]. All trajectories are generated by Qwen3-VL-32B-Thinking [19] acting as the teacher model. $\sim 25\%$ of the trajectories contain at least one tool call; the remainder solve the problem with internal reasoning alone. We retain only trajectories whose final answer is correct against the ground-truth label.

RL data composition. RL uses 15,591 problems obtained by filtering the SFT problem set: we remove problems that the SFT checkpoint solves on all 4 rollouts, and problems that the 32B teacher fails on all 4 rollouts. This filtering convention follows prior agentic RL work [23, 26] and removes both trivial problems (zero learning signal) and unreachable problems (no positive signal achievable at this scale). We additionally include 22,000 hard questions from MMFineReason-hard² to expose the policy to problems unseen during SFT, bringing the RL training set to $\sim 37\text{K}$ problems.

Policy gradient objective. Both SFT + GRPO and SFT + AXPO *maximize* the standard PPO-clip surrogate [32] regularized by a KL penalty toward a fixed reference policy π_{ref} (the SFT-initialized checkpoint). Letting $\rho_t(\theta) = \pi_\theta(y_t | \mathbf{x}, \mathbf{y}_{<t}) / \pi_{\theta_{\text{old}}}(y_t | \mathbf{x}, \mathbf{y}_{<t})$ denote the per-token importance ratio against the rollout policy $\pi_{\theta_{\text{old}}}$ and \hat{A} the trajectory-level advantage broadcast uniformly to every token of \mathbf{y} ,

$$\begin{aligned} \mathcal{L}_{\text{clip}}(\mathbf{y}; \hat{A}) = & \mathbb{E}_t[\min(\rho_t(\theta) \hat{A}, \text{clip}(\rho_t(\theta), 1 - \epsilon_{\text{low}}, 1 + \epsilon_{\text{high}}) \hat{A}) \\ & - \beta D_{\text{KL}}[\pi_\theta(\cdot | \mathbf{x}, \mathbf{y}_{<t}) \| \pi_{\text{ref}}(\cdot | \mathbf{x}, \mathbf{y}_{<t})]]. \end{aligned} \quad (6)$$

The training objective is $\max_\theta \mathbb{E}_{\mathbf{y} \sim \pi_{\theta_{\text{old}}}} [\mathcal{L}_{\text{clip}}(\mathbf{y}; \hat{A})]$. GRPO instantiates $\hat{A} = A_i$ for trajectory τ_i from [Section 2.1](#); AXPO applies the same surrogate per stream in [Equation 5](#) (per-prefix advantage on continuations, recovery-indicator advantage on the source prefix). We use the asymmetric DAPO clipping range $\epsilon_{\text{low}} = 0.2$, $\epsilon_{\text{high}} = 0.4$ and KL coefficient $\beta = 1 \times 10^{-3}$.

Hyperparameters. We adopt the ProRL [26] recipe for the RL stage. The key hyperparameters are:

- Sampling temperature: 1.0
- KL coefficient: 1×10^{-3}
- Asymmetric clipping: $\epsilon_{\text{low}} = 0.2$, $\epsilon_{\text{high}} = 0.4$ (DAPO-style [25])
- Group size: $N = 8$ rollouts per question
- Maximum number of turns per trajectory: 3
- Hardware: $8 \times$ A100 80GB GPUs

²A question subset of the MMFineReason corpus that Qwen3-VL-4B entirely fails on 4 rollouts.

All hyperparameters are held constant between SFT + GRPO and SFT + AXPO; only the rollout loop differs (see below).

For implementation of the training pipeline, we used verl [60] and rllm [61] libraries.

AXPO-specific hyperparameters. AXPO adds two knobs on top of the GRPO recipe:

- Branching budget: $r = 0.25$ of total rollout (i.e., extra continuations per training step are capped at $0.25 \cdot BN$).
- Per-prefix resample count: $K = 4$ continuations per selected prefix.

A.2. System Prompt and Tool Interface

We use the same agentic system prompt for SFT, RL, and evaluation across all model sizes where the prompt is modified version of the system prompt of deepeyes v2 [23]. Tools are exposed via a unified `<tool_call>` interface used in qwen-agent [19] and the model is free to invoke any subset of the three tools (`python`, `tavily-search`, `image_zoom_in`) on every question. The full text of the prompt is reproduced below.

System Prompt

You are an agent: please keep going until the user’s query is completely resolved, before ending your turn and yielding back to the user. Only terminate your turn when you are sure that the problem is solved.

Solve the following problem step by step. In your reasoning process, if the answer cannot be determined, you can write Python code in a Jupyter Notebook to process the image and extract more information from it. The stdout and stderr content, along with the images generated by “`plt.show()`” will be returned to better assist with the user query.

You MUST use the python tool to analyze or transform images whenever it could improve your understanding. This includes but is not limited to zooming in, rotating, adjusting contrast, computing statistics, or isolating features. If you find you lack sufficient knowledge to confidently answer the question, you MUST conduct search to thoroughly seek the internet for information. No matter how complex the query, you will not give up until you find the corresponding information. You can use the tavily-search tool, which will search the web and return relevant information based on your query.

Notes for tools:

image_zoom_in tool

1. **image_zoom_in** crops and magnifies a specific region of the image so you can inspect fine details.
2. When you need to look at a specific region more closely, prefer **image_zoom_in** over writing python code to crop — it is simpler, faster, and returns a high-resolution view directly.
3. After a zoom-in, the cropped image is appended to `_pil_images` in the python tool (the observation will tell you the exact index), so you can further process it with code if needed.

python tool

1. **python** runs in a stateful Jupyter notebook kernel — variables, imports, and state persist across calls.
2. The conversation images are pre-loaded as `_pil_images` (list of PIL Image objects) and `_images` (list of file paths). Images produced by other tools (e.g. `image_zoom_in`) are also appended to these lists.

3. Use `plt.show()` to visualize processed images; generated plots are automatically captured and returned.
4. Available packages include `numpy`, `scipy`, `sympy`, `matplotlib`, `PIL/Pillow`, and the standard library.
5. **Always use Python for non-trivial computation** — trigonometric calculations, multi-step arithmetic, equation solving, and area/volume formulas. Do NOT compute these mentally; write code to ensure numerical accuracy.
6. Your program should always return in finite time. Do not write infinite loops.
7. Writing file to disk is not allowed.

tavily-search tool

1. You MUST engage in many interactions, delving deeply into the topic to explore all possible aspects until a satisfactory answer is found.
2. Before presenting a Final Answer, you will **cross-check** and **validate the information** you've gathered to confirm its accuracy and reliability.
3. You will carefully analyze each information source to ensure that all data is current, relevant, and from credible origins.

general

You MUST think and plan before each function call, and reflect on the outcomes of the previous function calls. DO NOT do this entire process by making function calls only, as this can impair your ability to solve the problem and think insightfully.

Remember to place the final answer in the last part using the format:

```

<answer>
\boxed{"The final answer goes here."}
</answer>

```

Tool schemas. Each tool is registered with the model using the OpenAI function-calling schema (`name`, `description`, `JSON parameters`) and is concatenated with the system prompt above at every step. The three schemas in full are below.

python.

```

{
  "type": "function",
  "function": {
    "name": "python",
    "description": "Execute Python code in a persistent Jupyter kernel. State (variables,
      ↪ imports) is preserved across calls. Returns stdout/stderr and captured
      ↪ images. Conversation images are pre-loaded as `_pil_images` (list of
      ↪ PIL.Image) and `_images` (list of file paths). Use `_pil_images[0]` to access
      ↪ the first image directly - do NOT use plt.imread() or open files manually.",
    "parameters": {
      "type": "object",
      "properties": {
        "code": {
          "type": "string",
          "description": "Python code to execute in the sandbox environment."
        }
      },
      "required": ["code"],
      "timeout": {
        "type": "integer",

```

```

        "description": "Maximum execution time in seconds before timing out",
        "default": 12
    }
},
"required": ["code"]
}
}
}

```

image_zoom_in.

```

{
  "type": "function",
  "function": {
    "name": "image_zoom_in",
    "description": "Zoom in on a specific region of an image by cropping it based on a
        ↪ bounding box (bbox) and an optional object label",
    "parameters": {
      "type": "object",
      "properties": {
        "bbox_2d": {
          "type": "array",
          "items": {"type": "number"},
          "minItems": 4,
          "maxItems": 4,
          "description": "The bounding box of the region to zoom in, as [x1, y1, x2, y2]
              ↪ in 0-1000 relative coordinates, where (x1, y1) is the top-left corner
              ↪ and (x2, y2) is the bottom-right corner"
        },
        "label": {
          "type": "string",
          "description": "The name or label of the object in the specified bounding box"
        },
        "img_idx": {
          "type": "number",
          "description": "The index of the image to zoom in on (starting from 0)",
          "default": 0
        }
      }
    },
    "required": ["bbox_2d", "label"]
  }
}
}

```

tavily-search.

```

{
  "type": "function",
  "function": {
    "name": "tavily-search",
    "description": "Search the web for information on a specific query",
    "parameters": {
      "type": "object",
      "properties": {

```

```

    "query": {
      "type": "string",
      "description": "The search query"
    },
    "max_results": {
      "type": "integer",
      "description": "Maximum number of search results to return. Defaults to 5."
    }
  },
  "required": ["query"]
}
}
}

```

Search domain blacklist. To prevent answer leakage during training and evaluation, `tavily-search` is configured with the API-level parameter `exclude_domains = ["huggingface.co"]`, which filters out the site most likely to index benchmark questions or solutions. The exclusion is enforced uniformly across training and evaluation rollouts.

A.3. Benchmark Details

We evaluate on nine multimodal benchmarks grouped by which tool family is most expected to help: **Reasoning** (Python interpreter), **Perception** (image zoom-in), and **Search** (web search). All benchmarks are evaluated in the agentic setting with the same tool interface used in training; the model is free to use any subset of the three tools or none at all on every question.

Reasoning. These benchmarks evaluate multi-step reasoning over text, math, and figures, where a Python interpreter is the natural tool for symbolic and numerical computation.

- **MathVision** [38]: competition-style math problems paired with diagrams (geometry, algebra, combinatorics). Answers are short numerical or symbolic expressions; we use the public mini test set containing 304 questions.
- **DynaMath** [39]: a benchmark of programmatically generated math questions with multiple parametric variants per seed problem. We evaluate on a single-variant slice (501 seed problems). The benchmark complements MathVision as it provides additional algorithmically generated problems spanning plane geometry, statistics, and other domains with diverse difficulty.
- **Math-VR** [40]: a mathematical visual reasoning benchmark introduced with CodePlot-CoT, in which problems are paired with diagrams (figures, plots, geometric constructions) that the model must inspect to compute the answer. The benchmark targets the regime where the visual content is load-bearing for the math derivation rather than decorative.

Perception. These benchmarks contain high-resolution images with information that is hard to read at the default vision encoder resolution. The image zoom-in tool is the natural recovery mechanism.

- **V*** [8]: a fine-grained visual-search benchmark in which the answer depends on a small object embedded in a complex scene. Designed to expose the failure of monolithic image encoders on high-resolution detail.

- **VisualProbe** [7]: a multimodal probing benchmark introduced with mini-o3, where each question targets a specific small region (text, sign, label) within a high-resolution scene. We use the *hard* subset, which selects questions Qwen3-VL-Thinking-8B fails without tools.
- **HR-Bench-4K and HR-Bench-8K** [41]: high-resolution single-image perception at 4096^2 and 8192^2 resolutions, respectively. Questions probe small text, distant objects, and fine textures; the two splits share a common question pool with images rescaled to the target resolution.

Search. These benchmarks require external knowledge that is unlikely to be in the model’s parametric memory or that requires multi-hop lookup. The Tavily web search API is the natural tool.

- **HR-MMSearch** [42]: high-resolution multimodal search questions whose answers are composed by chaining two or more web lookups (e.g., “in which year was the mayor of the city where this fashion designer was born”). The benchmark stresses both perception (identifying entities from the image) and multi-hop search composition.
- **MMSearch** [43]: an earlier multimodal search benchmark covering current-events questions whose answers depend on web content released after the model’s training cutoff. Predominantly single-hop, but answers are often time-sensitive.

Evaluation protocol. For all benchmarks, we draw four rollouts per question and report Pass@1 (per-question accuracy averaged over four rollouts) and Pass@4 (a question is correct if any of the four rollouts is correct). Final-answer matching against the gold label is performed by an exact match for math and multiple-choice question and F1 score for search questions. For benchmarks that are hard to evaluate with exact match (e.g., MMSearch), we use a llm-as-a-judge using gpt-5-mini model.

Evaluation hyperparameters.

- Sampling: temperature 0.7, top- p 0.8, top- k 20, presence penalty 1.5
- Rollouts per question: $N = 4$ (used for Pass@1 / Pass@4)
- Maximum agentic turns per trajectory: 5
- Maximum response length: 32,768 tokens

B. Additional Experimental Results

This section collects supplementary results that complement the main Experiments: tool utilization rates at evaluation (Appendix B.1), per-benchmark Pass@4 numbers (Appendix B.2), per-rollout variance for Pass@1 (Appendix B.3), a stage-by-stage decomposition of the SFT-then-RL recipe (Appendix B.4), generalization to an unseen tool (Appendix B.5), per-row analysis of the ablation table (Appendix B.6), per-row analysis of the comparison table (Appendix B.7), a comparison against prior agentic VLM systems (Appendix B.8), and a post-hoc justification of confidence as the prefix-ranking signal (Appendix B.9).

B.1. Tool Utilization Rates at Evaluation

Table 4 reports tool utilization (the fraction of evaluation rollouts that emit at least one `<tool_call>`) on each of the nine benchmarks, mirroring the structure of Table 1. Across all three trainable scales

Table 4 | **Tool utilization rate** (% , \uparrow) per benchmark, mirroring Table 1. Tool utilization is the fraction of evaluation rollouts that emit at least one `<tool_call>` on each benchmark. Non-agent rollouts (no tools) have tool utilization 0 by construction and are omitted; “Base” is the inference-only baseline with tools enabled. Best per column within each size block in **bold**.

Method	Reasoning			Perception				Search		Avg.
	Math Vision	Dyna Math	Math -VR	V*	Visual Probe	HRBen. -4K	HRBen. -8K	HR-MM Search	MM Search	
<i>Qwen3-VL-2B-Thinking</i>										
Base	78.3	86.4	76.7	94.8	99.1	87.5	93.0	92.8	97.3	89.5
GRPO	96.1	99.0	93.2	96.9	100.0	90.0	94.0	100.0	100.0	96.6
SFT	38.8	34.3	8.0	95.8	100.0	79.5	80.5	91.5	95.0	69.3
+ GRPO	54.6	30.7	17.1	90.1	100.0	72.0	80.5	94.1	97.0	70.7
+ AXPO (Ours)	63.8	63.9	27.1	99.0	100.0	93.0	93.0	98.7	99.0	81.9
<i>Qwen3-VL-4B-Thinking</i>										
Base	25.7	17.0	1.6	94.8	99.1	79.5	85.5	85.2	95.7	64.9
GRPO	2.3	2.4	0.0	65.4	90.6	36.5	42.5	35.1	63.0	37.5
SFT	53.9	38.9	10.6	94.8	100.0	75.5	83.5	93.1	97.7	72.0
+ GRPO	38.8	27.7	8.6	80.6	100.0	64.0	74.5	91.5	95.7	64.6
+ AXPO (Ours)	73.0	96.2	13.3	100.0	100.0	100.0	100.0	100.0	100.0	86.9
<i>Qwen3-VL-8B-Thinking</i>										
Base	62.2	50.7	22.5	94.8	100.0	84.5	85.0	94.4	98.7	77.0
GRPO	38.2	22.0	7.8	87.4	99.1	72.0	75.5	91.1	97.3	65.6
SFT	47.7	34.1	9.8	90.6	99.1	74.0	76.0	93.4	96.7	69.0
+ GRPO	46.1	30.7	7.6	92.1	99.1	73.0	78.0	97.0	97.7	69.0
+ AXPO (Ours)	75.7	63.9	29.1	99.0	100.0	90.0	92.0	98.4	98.3	82.9
<i>Qwen3-VL-32B-Thinking (inference-only baseline)</i>										
Base	51.6	36.5	15.1	94.8	100.0	75.0	77.5	94.8	97.3	71.4

(2B/4B/8B), SFT + AXPO produces the highest average tool utilization among trained methods (81.9 / 86.9 / 82.9), and the gap to SFT + GRPO grows with size only on benchmarks where tool use is load-bearing (e.g., MathVision, DynaMath, Math-VR at 8B: +30/ +33/ +22 pp), while on tool-saturated benchmarks (V*, VisualProbe, MMSearch) both methods sit near 100%. Thus AXPO improves both tool-use frequency *and*, as Figure 5b suggests, conditional tool-use quality. The matched-tool analysis does not rule out frequency effects but rather shows that gains remain even on the subset of questions where both SFT + GRPO and SFT + AXPO invoke the same tool family.

B.2. Per-Benchmark Pass@4 Results

The main manuscript reports Pass@1 in Table 1; Table 5 reports the corresponding Pass@4 numbers across the same nine benchmarks and four model sizes, with identical method ordering and bold/underline conventions. The two tables share an Average column, which is the basis for the headline numbers in Section 4.2 and the per-stage decomposition below.

B.3. Pass@1 Variance Across Independent Rollouts

Table 1 reports Pass@1 averaged over four rollouts per question for compactness. To quantify rollout-induced variance, we re-evaluate every (model, benchmark) cell with **four independent evaluation rollouts** (each itself an average over four rollouts per question, matching the main-table protocol) and report the resulting mean \pm std in Table 6. Per-cell std values fall in the 0.4–3.6 pp range for nearly all entries, with isolated outliers on the smallest (2B) and most variance-prone (HRBench-8K) settings. The column-averaged std for SFT + AXPO is 1.4 pp at 4B and 1.2 pp at

Table 5 | **Main results: Pass@4** (% , \uparrow) on **nine multimodal benchmarks**, grouped into three categories: Reasoning, Perception, and Search. All methods use **Qwen3-VL-Thinking** [19] at four sizes (2B, 4B, 8B, 32B). Base (tools, no training) is the inference-only baseline; the Non-agent (no tools) baseline is reported separately in Table 7. Best result per column within each size block is **bolded**; second-best is underlined. Δ rows show AXPO’s gain over SFT + GRPO, the strongest comparable training recipe where AXPO outperforms it in most of evaluations. Pass@1 results are reported in Table 1.

Method	Reasoning			Perception				Search		Avg.
	Math Vision	Dyna Math	Math -VR	V*	Visual Probe	HRBen. -4K	HRBen. -8K	HR-MM Search	MM Search	
<i>Qwen3-VL-2B-Thinking</i>										
Base	32.6	76.6	28.9	81.7	15.1	79.0	77.0	18.7	46.3	50.7
GRPO	53.3	78.2	52.0	80.6	43.4	75.5	72.5	<u>29.5</u>	54.7	60.0
SFT	53.0	<u>80.2</u>	49.2	<u>91.1</u>	<u>50.0</u>	<u>86.5</u>	88.0	28.5	53.7	64.5
+ GRPO	<u>55.9</u>	<u>80.2</u>	<u>58.0</u>	94.2	60.4	83.5	<u>85.5</u>	28.2	<u>55.7</u>	<u>66.8</u>
+ AXPO (Ours)	61.2	83.6	60.0	94.2	60.4	88.5	88.0	33.4	57.3	69.6
Δ vs. SFT + GRPO	+5.3	+3.4	+2.0	+0.0	+0.0	+5.0	+2.5	+5.2	+1.6	+2.8
<i>Qwen3-VL-4B-Thinking</i>										
Base	64.8	82.6	65.1	<u>95.8</u>	44.3	83.5	81.0	27.5	55.7	66.7
GRPO	69.1	84.2	70.5	92.7	48.1	87.0	85.5	22.0	42.0	66.8
SFT	69.4	<u>86.4</u>	69.5	95.3	51.9	<u>89.5</u>	<u>88.0</u>	35.7	59.7	<u>71.7</u>
+ GRPO	<u>69.7</u>	85.8	71.9	97.9	<u>57.5</u>	88.0	84.5	<u>33.1</u>	<u>57.0</u>	<u>71.7</u>
+ AXPO (Ours)	74.3	87.0	72.1	97.9	65.1	91.0	90.0	32.1	<u>57.0</u>	74.1
Δ vs. SFT + GRPO	+4.6	+1.2	+0.2	+0.0	+7.6	+3.0	+5.5	-1.0	+0.0	+2.3
<i>Qwen3-VL-8B-Thinking</i>										
Base	63.5	85.2	68.3	92.7	55.7	85.5	82.5	33.8	59.0	69.6
GRPO	69.7	84.6	70.3	94.2	62.3	87.0	82.0	34.4	60.0	71.6
SFT	71.4	<u>86.0</u>	72.1	93.7	57.5	90.5	<u>87.0</u>	36.4	55.3	72.2
+ GRPO	<u>75.0</u>	87.0	74.3	96.9	<u>63.2</u>	87.5	84.5	<u>38.0</u>	<u>59.3</u>	<u>74.0</u>
+ AXPO (Ours)	75.7	87.0	<u>74.1</u>	<u>95.3</u>	67.9	<u>90.0</u>	89.0	42.0	61.0	75.8
Δ vs. SFT + GRPO	+0.7	+0.0	-0.2	-1.6	+4.7	+2.5	+4.5	+4.0	+1.7	+1.8
<i>Qwen3-VL-32B-Thinking (inference-only baseline)</i>										
Base	73.0	89.4	73.9	97.4	64.2	90.5	90.0	38.0	59.3	75.1

8B, both below the AXPO – SFT + GRPO Pass@1 deltas reported in Table 1 (+1.4 and +1.8 pp respectively), so the headline gains lie above the per-rollout noise floor.

B.4. Decomposing the SFT-then-RL Recipe

Table 5 contains four pre-AXPO baselines per model size: Base (tools, no training), GRPO (RL from base), SFT (SFT only), and SFT + GRPO. We additionally report a Non-agent (no tools, no training) configuration in Table 7 as a sanity check on the marginal value of inference-time tool access, which is orthogonal to the agentic-RL story. Reading the average Pass@1 / Pass@4 columns across these baselines isolates the contribution of each pipeline stage and motivates the SFT-then-RL recipe that AXPO builds on. All numbers in this section come from the **Average** columns of Table 1 (Pass@1) and Table 5 (Pass@4).

Why is post-training needed at all?

Comparing Non-agent and Base at the same model size measures the effect of *turning tools on without any training*. The gain is strongly scale-dependent: Pass@1 / Pass@4 deltas are -1.3 / +1.1at 2B, +5.2 / +9.2at 4B, +4.7 / +9.8at 8B, and +6.7 / +10.1at 32B. At 2B the Base (agentic) baseline is actually *worse* than the Non-agent baseline on Pass@1, showing that small models pay an agent-prompt overhead that outweighs the gain from

Table 6 | **Pass@1 mean \pm std** ($\%$, \uparrow) across **four independent rollouts** on nine multimodal benchmarks. Subscripts denote standard deviation across the four rollouts. Variance is comparable across methods, with most std values in the 0.4–3.6 pp range; the column-averaged std for SFT + AXPO is 1.4 pp at 4B and 1.2 pp at 8B.

Method	Reasoning			Perception				Search		Avg.
	Math Vision	Dyna Math	Math -VR	V*	Visual Probe	HRBen. -4K	HRBen. -8K	HR-MM Search	MM Search	
<i>Qwen3-VL-2B-Thinking</i>										
Base	18.6 \pm 1.8	60.5 \pm 1.2	16.9 \pm 1.5	63.0 \pm 2.9	5.0 \pm 1.4	64.6 \pm 0.9	55.9 \pm 0.5	8.2 \pm 1.5	27.7 \pm 1.4	35.6 \pm 1.5
GRPO	33.7 \pm 1.0	64.9 \pm 0.8	34.6 \pm 1.0	67.1 \pm 1.8	23.8 \pm 3.4	65.0 \pm 1.3	59.4 \pm 1.8	18.4 \pm 1.3	41.4 \pm 0.5	45.4 \pm 1.4
SFT	28.9 \pm 1.3	64.1 \pm 1.6	30.2 \pm 1.0	75.9 \pm 2.4	24.5 \pm 2.8	73.1 \pm 1.1	68.8 \pm 1.6	14.5 \pm 1.7	35.9 \pm 1.4	46.2 \pm 1.7
+ GRPO	34.8 \pm 1.3	66.4 \pm 1.0	35.8 \pm 2.2	81.7 \pm 3.2	36.1 \pm 1.5	74.2 \pm 0.8	70.6 \pm 2.1	15.7 \pm 1.0	40.6 \pm 1.2	50.7 \pm 1.6
+ AXPO (Ours)	35.0 \pm 1.1	66.9 \pm 2.2	38.9 \pm 1.0	81.3 \pm 3.1	35.1 \pm 5.0	77.9 \pm 1.9	72.4 \pm 1.6	18.1 \pm 0.4	40.2 \pm 1.7	51.8 \pm 2.0
<i>Qwen3-VL-4B-Thinking</i>										
Base	48.0 \pm 1.2	76.6 \pm 0.7	50.8 \pm 0.5	80.6 \pm 1.2	24.8 \pm 2.3	73.6 \pm 1.2	67.5 \pm 2.0	16.9 \pm 0.4	37.8 \pm 1.5	53.0 \pm 1.2
GRPO	52.5 \pm 2.3	76.2 \pm 1.0	57.9 \pm 1.1	82.7 \pm 2.8	29.7 \pm 1.9	75.5 \pm 1.3	71.1 \pm 1.5	12.7 \pm 1.2	23.8 \pm 1.7	53.6 \pm 1.6
SFT	49.1 \pm 1.3	76.3 \pm 1.0	55.3 \pm 1.2	87.0 \pm 1.9	34.7 \pm 1.7	79.5 \pm 1.3	74.1 \pm 1.0	20.6 \pm 1.7	41.5 \pm 1.5	57.6 \pm 1.4
+ GRPO	51.6 \pm 0.6	77.2 \pm 0.4	57.4 \pm 1.2	90.2 \pm 1.1	38.0 \pm 2.1	78.8 \pm 0.8	73.8 \pm 1.5	20.0 \pm 1.8	42.3 \pm 0.8	58.8 \pm 1.2
+ AXPO (Ours)	52.8 \pm 1.4	76.4 \pm 0.5	57.2 \pm 0.9	88.9 \pm 1.1	43.6 \pm 2.6	80.9 \pm 1.7	78.2 \pm 1.4	20.1 \pm 1.3	43.3 \pm 1.4	60.2 \pm 1.4
<i>Qwen3-VL-8B-Thinking</i>										
Base	47.1 \pm 2.0	75.9 \pm 0.9	54.9 \pm 1.1	77.7 \pm 2.2	31.8 \pm 1.8	72.8 \pm 1.7	66.1 \pm 2.2	21.0 \pm 1.0	42.7 \pm 1.7	54.4 \pm 0.6
GRPO	54.4 \pm 0.7	77.2 \pm 0.4	58.9 \pm 1.4	85.7 \pm 1.3	40.1 \pm 3.2	77.1 \pm 2.2	73.9 \pm 0.5	20.6 \pm 1.7	45.1 \pm 0.6	59.2 \pm 1.3
SFT	50.9 \pm 0.7	76.8 \pm 0.6	58.4 \pm 1.9	84.8 \pm 2.0	38.4 \pm 3.1	79.5 \pm 0.6	74.4 \pm 2.3	23.0 \pm 1.6	40.6 \pm 2.2	58.5 \pm 1.7
+ GRPO	55.3 \pm 1.8	78.2 \pm 1.0	60.4 \pm 1.5	87.7 \pm 2.4	40.1 \pm 3.6	79.5 \pm 1.1	74.9 \pm 1.1	24.4 \pm 1.2	44.0 \pm 0.4	60.5 \pm 0.5
+ AXPO (Ours)	56.1 \pm 1.4	79.0 \pm 0.9	60.6 \pm 0.8	87.8 \pm 0.4	45.8 \pm 1.1	83.2 \pm 0.6	77.0 \pm 4.3	25.9 \pm 0.7	45.0 \pm 0.4	62.3 \pm 1.2
<i>Qwen3-VL-32B-Thinking (inference-only baseline)</i>										
Base	56.5 \pm 1.4	83.3 \pm 0.6	64.1 \pm 1.1	89.1 \pm 1.1	40.3 \pm 2.4	85.2 \pm 1.6	78.9 \pm 3.7	22.8 \pm 1.2	46.1 \pm 1.6	62.9 \pm 1.6

correct tool use. Larger models recover Pass@1 and accumulate a Pass@4 ceiling gain, but even at 32B the gap to SFT + AXPO at 8B on Pass@4 (75.8 vs. 75.1) shows that inference-time tool access alone does not close the agentic gap. Post-training is therefore necessary at every trainable scale.

Why SFT before RL? Comparing GRPO (RL from base) against SFT + GRPO measures the value of an SFT initialization before RL. Pass@1 gaps shrink with size (+5.3 at 2B, +5.2 at 4B, +1.3 at 8B), but Pass@4 gaps remain positive at every scale (+6.8, +4.9, +2.4). RL from the base policy can find a single high-reward mode (Pass@1 partially recovered at 8B), but it consistently sacrifices diversity, capping the Pass@4 ceiling [62]. SFT broadens the cold-start distribution over tool-using trajectories before group-based exploration begins. Without it, all-wrong tool-using subgroups dominate from step 1 and the policy collapses onto a narrow single-mode solution [23].

Why RL after SFT? SFT minimizes log-likelihood on a fixed set of teacher trajectories: it can make the student *imitate* the teacher’s tool-use patterns, but the optimization signal lives entirely on the teacher’s distribution. At test time the student samples from its own distribution and small token-level deviations from the teacher accumulate into prefixes the SFT objective never scored, so imitation alone does not guarantee that on-policy rollouts inherit the teacher’s correctness (*exposure bias*). RL after SFT narrows this gap by training on the policy’s own rollouts under an outcome reward, adapting the policy to its own induced trajectory distribution rather than to the teacher’s [63]. Empirically, comparing SFT against SFT + GRPO isolates this on-policy adaptation effect given the SFT initialization: Pass@1 improves at every scale (+4.5 at 2B, +1.2 at 4B, +2.0 at 8B), the regime where on-policy reliability matters most, while Pass@4 gains are smaller and uneven (+2.3, +0.0, +1.8), consistent with GRPO consolidating mass on trajectories the SFT policy can already reach rather than discovering new ones. RL is therefore necessary on top of SFT, but standard GRPO’s adaptation is biased toward the SFT manifold, motivating AXPO’s tool-call resampling.

Table 7 | **Non-agent vs Base**: effect of turning tools on without any training, across nine multimodal benchmarks and four model sizes. *Non-agent* disables tool calls (the model answers from internal reasoning alone). *Base* enables the same tool interface as the trained methods but receives no post-training. Both Pass@1 and Pass@4 (% , \uparrow) are reported. The Pass@1 / Pass@4 deltas isolate the marginal value of inference-time tool access at each scale, motivating the post-training pipeline analyzed in [Appendix B.4](#).

Method	Reasoning			Perception				Search		Avg.
	Math Vision	Dyna Math	Math -VR	V*	Visual Probe	HRBen. -4K	HRBen. -8K	HR-MM Search	MM Search	
<i>Pass@1</i>										
<i>Qwen3-VL-2B-Thinking</i>										
Non-agent	27.9	66.5	24.8	64.8	18.2	57.8	57.3	5.1	9.5	36.9
Base	18.6	60.5	16.9	63.0	5.0	64.6	55.9	8.2	27.7	35.6
<i>Qwen3-VL-4B-Thinking</i>										
Non-agent	44.8	76.1	45.9	79.6	21.9	74.4	68.1	6.1	13.3	47.8
Base	48.0	76.6	50.8	80.6	24.8	73.6	67.5	16.9	37.8	53.0
<i>Qwen3-VL-8B-Thinking</i>										
Non-agent	52.5	75.5	50.6	78.0	27.6	70.8	68.1	8.5	15.3	49.7
Base	47.1	75.9	54.9	77.7	31.8	72.8	66.1	21.0	42.7	54.4
<i>Qwen3-VL-32B-Thinking</i>										
Non-agent	61.2	84.2	64.2	84.4	24.8	81.4	74.4	11.2	19.8	56.2
Base	56.5	83.3	64.1	89.1	40.3	85.2	78.9	22.8	46.1	62.9
<i>Pass@4</i>										
<i>Qwen3-VL-2B-Thinking</i>										
Non-agent	43.8	79.4	39.4	77.5	31.1	73.0	75.5	10.2	16.3	49.6
Base	32.6	76.6	28.9	81.7	15.1	79.0	77.0	18.7	46.3	50.7
<i>Qwen3-VL-4B-Thinking</i>										
Non-agent	62.0	82.6	60.4	89.0	31.1	83.5	78.5	9.8	20.3	57.5
Base	64.8	82.6	65.1	95.8	44.3	83.5	81.0	27.5	55.7	66.7
<i>Qwen3-VL-8B-Thinking</i>										
Non-agent	70.7	85.0	63.7	85.3	38.7	79.0	77.0	16.4	22.7	59.8
Base	63.5	85.2	68.3	92.7	55.7	85.5	82.5	33.8	59.0	69.6
<i>Qwen3-VL-32B-Thinking</i>										
Non-agent	78.9	91.2	75.3	91.6	33.0	88.5	80.5	16.4	30.0	65.0
Base	73.0	89.4	73.9	97.4	64.2	90.5	90.0	38.0	59.3	75.1

Why AXPO on top of SFT, instead of GRPO? The previous two paragraphs leave a structural gap: SFT sets the Pass@4 ceiling and RL sharpens within it, so further gains require a mechanism that simultaneously extends the ceiling *and* sharpens. AXPO does both. Pass@1 gains over SFT + GRPO are +1.1/ +1.4/ +1.8 at 2B/4B/8B, and Pass@4 gains are +2.8/ +2.3/ +1.8. The Pass@4 lift is the diagnostic signature that AXPO operates on a different axis from SFT-then-GRPO sharpening: by recovering all-wrong tool-using subgroups whose gradient signal would otherwise vanish ([Section 2.2](#)), AXPO turns previously dead continuations into trainable ones, expanding the policy’s reachable correct-trajectory set rather than only redistributing mass within it.

B.5. Generalization to an Unseen Tool: Image Search

Training in [Section 4.1](#) uses three tool families: a Python interpreter, a Tavily web search engine, and an image zoom-in tool. None of these is an *image-based* retrieval tool that takes an image as the query and returns visually similar pages, which we cannot directly utilize due to excessive API costs.

Table 8 | **Generalization to an unseen tool.** MMSearch Pass@1 / Pass@4 (% , \uparrow), with and without an image-search tool added at inference time. Image search is not in the training tool set (Python, Tavily web search, image zoom-in). AXPO converts the new tool into Pass@1 gains more effectively than GRPO (+4.6 pp vs. +2.8 pp), while Pass@4 gains are similar across the two methods.

		SFT + GRPO	SFT + AXPO
w/o image search	Pass@1	44.0	45.0
	Pass@4	59.3	61.0
w/ image search	Pass@1	46.8	49.6
	Pass@4	65.3	66.7

To probe whether AXPO’s tool-using policy transfers beyond the training tool inventory, we extend the inference-time tool set with an image-search tool and re-evaluate on **MMSearch** [43], the search benchmark with the largest fraction of image-grounded queries. Since we did not have access to a production image-retrieval endpoint at the budget required for full evaluation, we approximate the tool by prompting GPT-5.4 with the query image and instructing it to return the kind of structured response a visual-search API would emit (caption, candidate entity names, related URLs). This proxy is imperfect, but it preserves the key property the experiment probes: an entirely new tool interface, unseen at training time, whose output the model must integrate into its reasoning.

Table 8 shows the result. *Without* image search at inference, SFT + GRPO and SFT + AXPO are essentially tied (Pass@1: 44.0 vs. 45.0; Pass@4: 59.3 vs. 61.0). *With* image search at inference, the gap opens on Pass@1: AXPO gains +4.6 pp (45.0 \rightarrow 49.6) while GRPO gains only +2.8 pp (44.0 \rightarrow 46.8); on Pass@4 both methods gain similarly (+6.0 and +5.7). The Pass@1 asymmetry suggests AXPO not only *can* use the unseen tool when given enough samples (Pass@4 captures this) but converts that capability into reliable first-shot answers, whereas GRPO’s tool-using policy is more narrowly fitted to the training tool inventory. We read this as evidence that resampling-induced exposure to diverse tool-call resolutions during training transfers to tool families the model has never been trained on, although the claim is bounded to one benchmark and one new tool type.

B.6. Detailed Ablation Analysis

Table 2 ablates each AXPO design choice on 8B at matched compute. All numbers below are 8B Pass@1 averages on the four-benchmark composition (MathVision, V*, VisualProbe, HR-MMSearch).

Prefix fixing. Removing prefix fixing reduces AXPO to 52.1, near the SFT + GRPO baseline of 51.9: each resample becomes a fresh rollout from $\pi_\theta(\cdot | \mathbf{x})$, so only a q -fraction of resamples are tool-using and the $(1-q)$ waste factor that Proposition 1 removes returns in full.

Tool-using resampling target. Targeting questions where all no-tool rollouts fail for resampling instead reaches 51.7, since the policy already covers the no-tool subgroup under GRPO and additional samples there cannot recover the missing tool-using signal. Resampling pays off only when the resampling target is the under-covered tool-using subgroup.

Uncertainty-based prefix selection. Replacing uncertainty rank with random ranking drops to 51.0 (−2.9 pp): the prefix is still fixed so the coverage gain is preserved, but random ranking routes the budget to prefixes where the policy has already converged toward a wrong continuation, wasting resamples on determined commitments.

Prefix credit. Dropping the recovery-indicator credit on the source prefix yields 51.4 (−2.5 pp): prefix tokens receive no positive signal even when resampling recovers a continuation, so the policy is not steered toward producing high-yield prefixes in the first place.

Per-prefix advantage group. Merging resampled continuations into the source group instead of forming a per-prefix advantage yields 51.2 (−2.7 pp): the shared prefix then collects contradictory advantages from the failed source and successful resamples while no-tool successes in the source group dilute the recovered signal.

B.7. Detailed Comparison Analysis

Table 3 compares AXPO to alternative training recipes. All numbers are 8B Pass@1 averages.

Reward shaping does not recover the gain of AXPO. A tool penalty [29] drops to 46.0 and a tool bonus [18, 44, 45] reaches only 50.8, both *below* the GRPO baseline of 51.9. Reward-channel interventions either suppress tool use globally (penalty) or reward tool calls regardless of whether they help (bonus); neither addresses the coverage problem that AXPO targets, which is conditional on the prefix being tool-using and on resampling restoring at least one correct continuation.

Extra rollout budget does not close the gap. Doubling the GRPO rollout count ($\times 4$ exceeding AXPO’s extra compute) reaches 52.4, still 1.5 pp below SFT + AXPO. The extra budget re-derives non-tool-using prefixes and cannot break the all-wrong tool-using subgroups that resampling is designed to recover; throwing more samples at the same $(1-q)$ waste factor does not change the structural problem.

Alternative RL algorithms. We replace GRPO with three recently proposed alternatives. RLTF [46], an algorithm that utilizes the text feedback from the external teacher, reaches only 43.3 Avg with 40% tool utilization, suffering tool-call collapse over training (consistent with reports of hint leakage degrading text-feedback RL on agentic tasks). CISPO [47], an importance-sampling variant, reaches 47.8 Avg: its clip rule reduces gradient bias but does not address the all-wrong subgroup whose advantage is zero by construction. ARPO [31], an agent-specific branching method that draws additional continuations after a tool observation when post-observation entropy is high, is the closest comparison and the strongest competitor at 51.3 Avg, yet still trails AXPO by 2.6 pp: post-observation branching cannot recover when the tool call itself is the failure mode, which is the regime Section 2.2 identifies as binding. The RL-algorithm sweep confirms AXPO’s gain is not a generic effect of any agent-aware RL trick but specifically reflects tool-call resampling’s coverage restoration on tool-using thinking prefixes.

B.8. Comparison with Prior Agentic VLMs

Table 9 situates SFT + AXPO against prior agentic VLM systems on the five benchmarks for which their published numbers are available (MathVision, DynaMath, V*, HR-Bench-4K, HR-Bench-8K) from previous work [18, 23]. This comparison is not strictly controlled: prior systems use different base models (mostly Qwen2.5-VL-7B), different training dataset scale, and report on benchmark subsets, so part of any gap reflects base-model improvements rather than method choice. With that caveat, SFT + AXPO at 8B leads on four of the five benchmarks and on the cross-benchmark average (76.6 vs. 66.3 for the strongest prior system reporting on all five). The exception is V*, where

Table 9 | Comparison with prior agentic VLM systems on five benchmarks where numbers are publicly available. All numbers are Pass@1 (%). “–” indicates the method does not report on that benchmark. Average is computed only over methods with all five entries. Best per column is **bolded**; second-best is underlined. Prior agentic systems use different base models (mostly Qwen2.5-VL-7B), so absolute values are not strictly comparable; the Δ *vs. base* rows report each group’s best improvement over its own base, isolating the post-training gain from the base-model gap. AXPO delivers a larger average lift over its base (+8.7 pp) than the strongest prior agentic recipe over Qwen2.5-VL-7B (+6.9 pp).

Method	MathVision	DynaMath	V*	HR-Bench-4K	HR-Bench-8K	Avg.
<i>Qwen2.5-VL-7B base + prior agentic methods</i>						
Qwen2.5-VL-7B-Instruct [64]	25.6	53.3	78.5	71.6	67.9	59.4
PixelReasoner [44]	–	–	84.3	74.0	66.9	–
Mini-o3 [7]	–	–	<u>88.2</u>	77.5	73.3	–
DeepEyes [45]	26.6	55.0	85.6	75.1	72.6	63.0
Thyme [58]	27.6	–	82.2	77.0	72.0	–
DeepEyes-v2 [23]	28.9	57.2	81.8	<u>77.9</u>	<u>73.8</u>	–
PyVision-RL [18]	28.7	61.6	88.7	78.1	74.3	66.3
Δ <i>vs. base (best prior)</i>	<i>+3.3</i>	<i>+8.3</i>	<i>+10.2</i>	<i>+6.5</i>	<i>+6.4</i>	<i>+6.9</i>
<i>Qwen3-VL-8B-Thinking base + ours</i>						
Qwen3-VL-8B-Thinking (Agent) [19]	<u>47.1</u>	<u>75.9</u>	77.7	72.8	66.1	<u>67.9</u>
SFT + AXPO (Ours)	56.1	79.0	87.8	83.3	77.0	76.6
Δ <i>vs. base (ours)</i>	<i>+9.0</i>	<i>+3.1</i>	<i>+10.1</i>	<i>+10.5</i>	<i>+10.9</i>	<i>+8.7</i>

pixel-level reasoning systems (Mini-o3, PyVision-RL) sit within ~ 1 pp; this is a benchmark where image zoom-in is the load-bearing tool and tool-using rollouts are already near saturation across systems, so the headroom for gradient-rescue is small. The largest gaps appear on math-over-image benchmarks (MathVision, DynaMath), where prior agentic VLM training has invested less and where AXPO’s tool-call gradient survival is most directly load-bearing.

B.9. Confidence as a Tractable Proxy for Tool-Call Entropy

Section 3 ranks candidate prefixes by the mean probability the source policy assigned to the tool-call tokens of τ^{src} (henceforth *confidence*). The natural alternative is the predictive entropy $H(\pi_\theta(\cdot | \mathbf{x}, \mathbf{y}_{<t}))$ of the next-token distribution at each tool-call position, but this choice is precluded by training-loop structure. Per-token sampling probabilities are emitted essentially for free by the rollout engine (vLLM [65]), whereas predictive entropy requires either an extra forward pass over the full vocabulary under the trained policy (FSDP) or vLLM-side full-vocabulary logprob expansion at decode time. Our RL pipeline under verl [60] alternates rollout (vLLM) and gradient updates (FSDP), so inserting a per-prefix entropy computation would force an additional vLLM \rightarrow FSDP \rightarrow vLLM round-trip per training step (or equivalently expensive vLLM-side full-vocabulary logprob expansion), a cost we wished to avoid.

To verify that confidence preserves the ranking an entropy-based scheme would induce, we measured the per-step correlation between mean-token-confidence and exact policy entropy on tool-call positions of failed tool-using rollouts collected during training (Figure 6). Across training steps, the two signals are strongly correlated (Pearson $\rho = 0.843$, Spearman $\rho = 0.835$, OLS fit $y = 0.41x + 0.07$ on entropy vs negated confidence). Confidence therefore preserves the relative ordering an entropy-based scheme would produce, and we adopt it as the ranking signal in AXPO.

C. Extended Related Works

This appendix expands on Section 5 with the longer descriptions that the main text abridges.

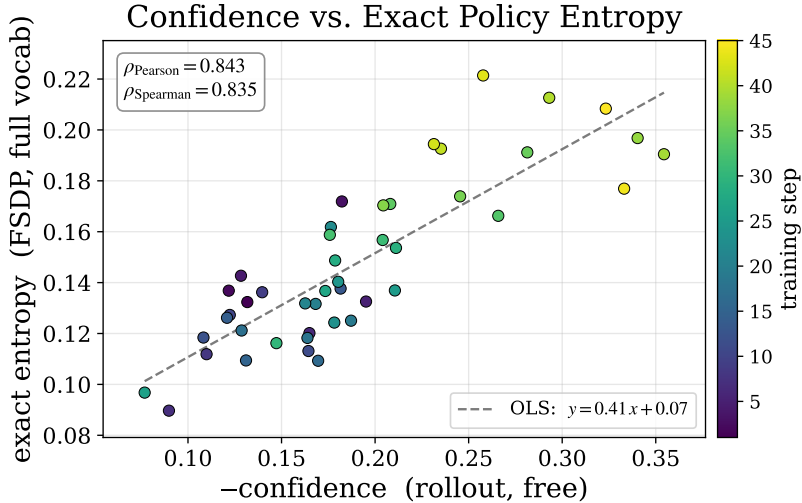


Figure 6 | **Confidence vs. exact policy entropy at tool-call positions.** For each training step, we plot the mean confidence (vLLM rollout, free) against the exact policy entropy (FSDP forward, full vocabulary) on tool-call tokens of failed tool-using rollouts. The two signals are strongly correlated (Pearson $\rho = 0.843$, Spearman $\rho = 0.835$), justifying confidence as a tractable uncertainty proxy.

Two-stage SFT-then-RL recipe for agentic VLMs. Recent agentic VLM systems share a two-stage recipe: supervised fine-tuning on tool-using trajectories distilled from larger teachers [66, 20], followed by outcome-reward RL [18, 23, 45]. They differ mainly in the distillation corpus, the tool interface, and the choice of base model. Most prior agentic-RL VLM studies focus on a single tool family (typically image manipulation), whereas our setup combines code, search, and image zoom-in on a thinking-capable base (Qwen3-VL-Thinking) [19], a configuration under which the RL stage becomes the primary bottleneck.

Group-relative RL and BroRL. RL with verifiable outcome rewards is the standard post-SFT stage for reasoning models [1, 2]. GRPO [24–26] samples N rollouts per question, normalizes rewards within the group, and assigns the resulting advantage uniformly to every token. BroRL [30] argues that increasing N reduces unsampled blind spots at a rate determined by per-token baseline probability. Both analyses were developed for thinking-only trajectories, where the rollout structure is uniform across tokens and the per-token baseline probability decays slowly. Proposition 1 shows that AXPO’s prefix-fixed resampling dominates raw scaling in the regime where tool-call tokens sit at low policy probability, exactly the failure mode Section 2.2 diagnoses.

Mid-trajectory branching for tool-using RL. ARPO [31] and AEPO [59] adapt group-relative RL to tool-using rollouts by branching *after* a tool observation, drawing additional continuations from $\pi_\theta(\cdot | \mathbf{x}, \mathbf{t}_1, \mathbf{a}_1, \mathbf{o}_1)$ when post-observation entropy is high. The exploration target is the continuation given a fixed tool call, which absorbs variance introduced by the tool output but cannot recover when the tool call itself is wrong (wrong sub-image, wrong python code, wrong search query). AXPO instead branches *at* the tool-call boundary and triggers only on all-wrong tool-using subgroups, with a per-prefix advantage that credits the source prefix exactly when its branched continuation succeeds, making it a targeted intervention on the regime Section 2.2 identifies as binding rather than a general rollout-budget reshapener. Empirically, AXPO outperforms ARPO on the 8B comparison (53.9 vs. 51.3 Avg, Table 3), consistent with the diagnosis that the tool call itself, not the post-observation continuation, is the dominant failure locus. The two strategies are compatible, and combining

tool-call and post-observation branching is a natural extension we leave to future work.

D. Coverage Argument for Tool-call resampling

This appendix formalizes [Proposition 1](#): prefix-fixed resampling from a tool-committed prefix dominates raw sampling at recovering correct tool-using rollouts whenever the selected prefix satisfies $p(\mathbf{t}_1) \geq qp^{\text{tool}}$, with strict inequality once $p(\mathbf{t}_1) > qp^{\text{tool}}$. The mechanism is $q \rightarrow 1$ by construction: every resampled continuation from a tool-committed prefix is tool-using, so raw’s $(1 - q)$ waste factor vanishes and the threshold a prefix must clear sits at qp^{tool} , strictly below the average per-tool-using-rollout success p^{tool} .

Setup. Let π_θ be the policy, \mathbf{x} a question, and $R(\tau) \in \{0, 1\}$ the outcome reward. Decompose $\tau = (\mathbf{t}_1, \mathbf{y}_{\geq 1})$ into a thinking prefix and its continuation (tool call, tool output, and the remainder of the trajectory). Let $\mathcal{T} = \{\mathbf{t}_1 : \mathbf{t}_1 \text{ includes the opening } \langle \text{tool_call} \rangle \text{ tag}\}$ be the set of tool-committed prefixes, and define

$$q := \Pr_{\pi_\theta}[\mathbf{t}_1 \in \mathcal{T} \mid \mathbf{x}], \quad p(\mathbf{t}_1) := \Pr_{\pi_\theta}[R = 1 \mid \mathbf{x}, \mathbf{t}_1], \quad p^{\text{tool}} := \mathbb{E}_{\mathbf{t}_1 \sim \pi_\theta(\cdot \mid \mathbf{x}, \mathbf{t}_1 \in \mathcal{T})}[p(\mathbf{t}_1)].$$

So q is the rate at which the policy commits to tool use from \mathbf{x} , and p^{tool} is the per-tool-using-rollout success rate. Both are directly measurable ([Figure 3a](#), [Figure 3b](#)). We compare two samplers, each drawing N trajectories, on the event “at least one sample is a correct tool-using rollout”:

- **Raw rollout:** $\tau \sim \pi_\theta(\cdot \mid \mathbf{x})$. Per-sample probability of a correct tool-using rollout is $\Pr[\mathbf{t}_1 \in \mathcal{T}] \cdot \Pr[R = 1 \mid \mathbf{t}_1 \in \mathcal{T}] = qp^{\text{tool}}$.
- **Prefix-fixed resampling:** fix $\mathbf{t}_1^{\text{src}} \in \mathcal{T}$ and draw continuations from $\pi_\theta(\cdot \mid \mathbf{x}, \mathbf{t}_1^{\text{src}})$. Every resampled continuation is tool-using by construction ($q \rightarrow 1$), and per-resample success is $p(\mathbf{t}_1^{\text{src}})$.

Coverage, i.e., the probability that at least one of the N samples is a correct tool-using rollout, equals $1 - (1 - p_{\text{eff}})^N$ with $p_{\text{eff}} = qp^{\text{tool}}$ under raw rollout and $p_{\text{eff}} = p(\mathbf{t}_1^{\text{src}})$ under resampling.

Proof of [Proposition 1](#). The function $f(p) = 1 - (1 - p)^N$ has derivative $f'(p) = N(1 - p)^{N-1}$, non-negative on $[0, 1]$ and strictly positive on $[0, 1)$, so f is non-decreasing on $[0, 1]$ and strictly increasing on $[0, 1)$. Under the assumption $p(\mathbf{t}_1^{\text{src}}) \geq qp^{\text{tool}}$, applying f to both sides gives $1 - (1 - p(\mathbf{t}_1^{\text{src}}))^N \geq 1 - (1 - qp^{\text{tool}})^N$. Strictness follows whenever $p(\mathbf{t}_1^{\text{src}}) > qp^{\text{tool}}$ and $qp^{\text{tool}} \in (0, 1)$. The mechanism is $q \rightarrow 1$ by construction: resampling eliminates raw’s wasted $(1 - q)$ fraction of non-tool rollouts, so the baseline threshold is qp^{tool} rather than p^{tool} .

Consequence for GRPO training. Under GRPO with binary rewards, coverage on correct tool-using rollouts determines whether tool-call tokens receive a *positive* (reinforcing) gradient. If the tool-using subgroup contains no correct rollout, the tool-call tokens get no positive signal: the subgroup is either empty (no tool-call tokens at all in the group) or all-wrong with non-positive group-normalized advantage — zero in fully all-wrong groups ($r_i - \text{mean}(\{r_j\}) = 0$) and *negative* in mixed-success groups where some no-tool rollouts succeed (which actively penalizes tool use). Hence $1 - (1 - p_{\text{eff}})^N$ is exactly the probability that a group produces a positive (reinforcing) learning signal at the tool call. [Proposition 1](#) then says that prefix-fixed resampling strictly breaks the all-wrong tool-using subgroups identified in [Figure 3b](#) at any fixed N .

Satisfying the threshold. By the definition of p^{tool} as the conditional expectation over the tool-committed prefix distribution $\pi_{\theta}(\cdot \mid \mathbf{x}, \mathbf{t}_1 \in \mathcal{T})$, $\mathbb{E}_{\mathbf{t}_1}[p(\mathbf{t}_1)] = p^{\text{tool}} > qp^{\text{tool}}$ whenever $q < 1$, so the expected prefix lies strictly above the [Proposition 1](#) threshold. All prefixes at or above the conditional mean satisfy the assumption, and so do below-average prefixes down to qp^{tool} ; only prefixes with strongly subpar per-branch success ($p(\mathbf{t}_1) < qp^{\text{tool}}$) can underperform raw sampling. Empirically, $p(\mathbf{t}_1)$ is far from constant across \mathcal{T} : fixing a failed tool-using rollout’s prefix and resampling its tool call recovers $\sim 15\%$ of originally-failed tool-using subgroups.

Relation to BroRL. Our target is tool use, and the diagnostics in [Section 2.2](#) establish exactly the regime where naive rollout scaling fails to help: tool use is rare ([Figure 3a](#): $q \in [0.2, 0.35]$) and all-wrong rates on tool-using subgroups are high ([Figure 3b](#)), so tool-call tokens sit in a low-probability regime under the policy. Hu et al. [30] show that scaling N reduces unsampled blind spots at rate $p^2(1-p)^N$ (Theorem 1, Lemma 2); this decay is per-token, fast for high- p regions and slow for low- p regions. Raw scaling therefore preferentially fills the thinking-only blind spot while leaving the tool-call blind spot under-sampled. [Proposition 1](#) sidesteps this by relocating samples: conditioning on a tool-committed prefix eliminates the $(1-q)$ waste factor so the local per-branch success becomes $p(\mathbf{t}_1^{\text{src}})$, and the same budget N reaches the tool region effectively. BroRL’s guarantee is uniform in token type; AXPO targets the specific region that the low tool-use attempt rate has made hardest to cover.

E. Limitations and Future Work

We expand on the limitations sketched in the main-text conclusion and discuss future directions.

Verifiable outcome rewards. AXPO’s subgroup-level trigger (“all-wrong tool-using subgroup”) and per-prefix advantage in [Eq. 2](#) both rely on a binary, automatically verifiable outcome signal $r \in \{0, 1\}$. Tasks where verifiability is partial (open-ended generation [67, 68], multi-criterion subjective evaluation) require a different definition of “failed subgroup” before tool-call resampling applies. The resampling mechanism itself is reward-agnostic, but the trigger and the all-wrong learning signal argument in [Section 2.2](#) are not.

Compute scope of training. Trained models are at most 8B parameters; 32B is reported inference-only as the SFT teacher. This boundary reflects available compute rather than a methodological choice [69, 68, 70–72]. Whether the Thinking-Acting Gap and AXPO’s recovery generalize to 32B+ trainable scale, where the base policy is closer to the tool-use ceiling and the all-wrong-subgroup fraction may be smaller, is open. Furthermore, although the teacher model can theoretically scale to 100B+ parameters, analyzing the effects of teacher scaling on downstream reinforcement learning (RL) remains an area for future work.

Future work: richer tool environments. Our tool inventory covers three families that span numerical, retrieval, and visual modalities (Python interpreter, web search, image zoom-in), each shown to be load-bearing in prior agentic VLM work [23, 18, 7]; this multi-tool setup is already broader than most prior agentic-VLM RL studies, which typically focus on a single tool family. One notable absence is an image-search tool, which prior works [23, 42] report results with but which we could not include during training and full evaluation due to per-call API costs at our scale (we instead approximate it via a GPT-5.4 prompt for the unseen-tool study in [Appendix B.5](#)). Tools with longer execution latency (browser agents, GUI control, terminal sessions) and tools with

high per-call cost (LLM-as-tool) [13] introduce additional considerations that we do not address. Extending AXPO to such richer [73–75], longer-horizon environments is a natural next step.

Future work: generalization to other base models. All experiments use Qwen3-VL-Thinking, which is currently the strongest open thinking-capable VLM with reliable tool-using ability and the model best supported by our RL framework. The Thinking-Acting Gap is a property of RL on an agentic reasoning model rather than of any specific architecture [76–79], and we expect the diagnostics and AXPO’s coverage gain to transfer; replicating on the most recent Qwen3.5 models [80], once RL framework support matures, would help establish the gap as a general phenomenon and rule out base-specific confounds.

F. Broader Impacts

AXPO is a methodological improvement to the RL training of agentic VLMs and is additive on top of a publicly released base model (Qwen3-VL-Thinking [19]), so it does not introduce a new capability class. Among the three tool families used in this work, the Python interpreter raises standard security concerns for code-executing agents. We can run all tool calls in a sandboxed execution environment during both training and evaluation, consistent with prior agentic-VLM RL work [12]. Beyond this sandboxing, broader safety considerations [81–87] (e.g., misuse of tool-grounded outputs, causality, robustness, deployment-time guardrails, downstream effects of cheaper agentic deployments) are out of scope for this work and were not addressed.

G. Qualitative Examples: GRPO vs. AXPO

We show three side-by-side trajectories where SFT + AXPO succeeds (4/4) and SFT + GRPO fails (0/4) at the 8B scale, one per modality (perception, reasoning, search). For each example we display the question, the correct answer, and one representative trajectory per method. Thoughts are extensively abbreviated with ellipses for brevity; tool calls and outputs are reproduced verbatim.

G.1. Perception: tiny-text reading on a Hong Kong street scene

Question

Benchmark: VisualProbe-hard [7]. **Ground truth:** 2563.

Prompt: “What is the number to the left of 1000?”



AXPO ✓

Step 0, <think>. “...checking phone numbers and license plates... looking at the yellow sign on the right side under SUNBEAM THEATRE, there’s a section with ‘Tel: 2563 1000’... Let me confirm with image_zoom_in.”

Step 0, <tool_call>.

```
image_zoom_in({"bbox_2d": [870, 450, 945, 517], "label": "Telephone number sign", "img_idx": 0})
```



Step 1, <think>. “The cropped image clearly shows ‘Tel: 2563 1000’. The number to the left of 1000 is 2563.”

<answer> 2563 ✓

GRPO ×

Step 0, <think>. “...checking traffic lights... license plates... bus route numbers... none match 1000... maybe the question is a trick. The number to the left of 1000 in numerical order is 999... Let me try image_zoom_in... [reasoning continues without ever emitting a tool call]... Given that this is a common math question, the answer is likely 999.”

No tool calls were emitted.

<answer> 999 ×

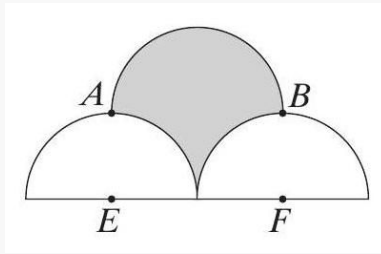
The thinking prefix in both rollouts identifies the right candidate region, but only AXPO commits to a tool call; GRPO talks itself into a numerical-order guess (999) and never invokes `image_zoom_in`, despite repeatedly mentioning it as a candidate action. All four GRPO rollouts on this question follow the same pattern.

G.2. Reasoning: geometry disambiguation via python visualization

Question

Benchmark: MathVision [38]. **Ground truth:** 8.

Prompt: “Three semi-circles as shown. $ABEF$ is a rectangle and the radius of each of the semi-circles is 2 cm. E and F are the centers of the bottom semi-circles. The area of the shaded region (in cm^2) is:”



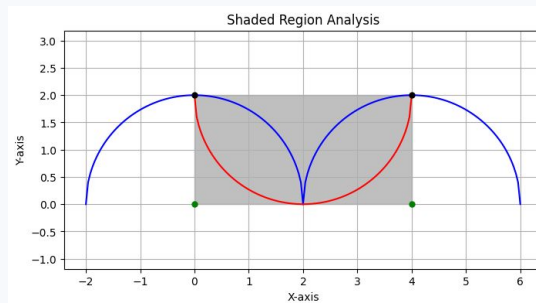
AXPO ✓

Step 0, <think>. “...Setting $E = (0, 0)$, $F = (4, 0)$, the top semicircle has center $(2, 2)$ and radius 2. Computing sector minus triangle for each side gives an overlap of $\pi - 2$... Shaded $= 2\pi - 2(\pi - 2) = 4$. The result matches the area of a 2×2 square, suggesting correctness. Let me also visualise the configuration to confirm.”

Step 0, <tool_call>.

```
python({"code": "import matplotlib.pyplot as plt; import numpy as np;...ax.plot(x1, np.sqrt(4-x1**2), 'b'); ax.plot(x2, np.sqrt(4-(x2-4)**2), 'b'); ax.plot(x3, 2-np.sqrt(4-(x3-2)**2), 'r'); ax.add_patch(plt.Polygon([(0,2),(0,0),(4,0),(4,2)], color='gray', alpha=0.5));..."})
```

Tool output (matplotlib figure).



Step 1, <think>. “...The plot shows the bottom semicircles curving **upward** from EF to A and B (forming quarter-disks at corners E, F , total area 2π) and the top semicircle curving **downward** from AB to $(2, 0)$ (a half-disk of area 2π). Since the two areas match, by area-swap the shaded region rearranges to the full rectangle $ABEF$: $4 \times 2 = 8$.”

<answer> 8 ✓

GRPO ✗

Step 0, <think>. "... Top semicircle area = 2π . Each side gives a sector of $\pi/2$ minus a right triangle of area 2, so each segment is $\pi - 2$. Subtracting both: $2\pi - 2(\pi - 2) = 4$ so the shaded area is 4."

No tool calls were emitted.

<answer> 4 ✗

Both rollouts begin with the same algebraic derivation that subtracts the two overlapping segments from the top semicircle and arrives at 4, the area of the wrong sub-region. The error is geometric, not arithmetic. AXPO emits a python call to render the configuration; the matplotlib output makes the area-swap structure visible – the bottom quarter-disks at corners E, F inside the rectangle (total area 2π) match the top half-disk hanging from AB (also 2π), so the shaded region rearranges to the rectangle area $8 = 4 \times 2$, and the model revises accordingly. All four GRPO rollouts emit zero tool calls and commit to one of the wrong values (4, 4, 4, 2π). The example illustrates a clean instance of the Thinking-Acting Gap: the algebraic prefix is sound but the area-swap intuition only becomes accessible after a tool call, and GRPO never learns to invoke it on questions of this type.

G.3. Search: multi-hop decomposition into two sequential queries

Question

Benchmark: HR-MMSearch [42]. **Ground truth:** 1984.

Prompt: "In which year was the mayor, who will be serving in August 2025, born in the city where the fashion designer of this fashion show was born?"



AXPO ✓

Step 0, <think>. "The backdrop reads PAUL COSTELLOE; designer is Paul Costelloe. I need (i) his birthplace, (ii) the mayor of that city in August 2025, (iii) the mayor's birth year. Start with the birthplace."

Step 0, <tool_call>.

```
tavily-search({"query": "Paul Costelloe birthplace", "max_results": 5})
```

Tool output (truncated). "... Born in Dublin, Ireland ... Paul Costelloe (23 June 1945 – 21 November 2025)..."

Step 1, <think>. "Birthplace = Dublin. Now the Lord Mayor of Dublin in August 2025."

Step 1, <tool_call>.

```
tavily-search({"query": "current mayor of Dublin Ireland 2024", "max_results": 5})
```

Tool output (truncated). "Ray McAdam (born 1984) is an Irish Fine Gael politician who

has served as Lord Mayor of Dublin since June 2025.”

Step 2, <think>. *“Designer was born in Dublin; Lord Mayor of Dublin since June 2025 is Ray McAdam, born 1984.”*

<answer> 1984 ✓

GRPO ×

Step 0, <think>. *“Designer is Paul Costelloe; born in Dublin in 1945. Mayor of Dublin in 2025 – the search results don’t directly show this, but if the riddle is that the mayor is the same age as the designer, the answer would be 1945.”*

Step 0, <tool_call>.

`tavily-search({"query": "Paul Costelloe birthplace", ...})`

Tool output (truncated). *“...Born in Dublin, Ireland ... Paul Costelloe (23 June 1945 – 21 November 2025)...”*

Step 1, <think>. *“... search returned the designer’s info but not the mayor’s. I’ll commit to 1945 since the designer was 80 in 2025 and the question may be a riddle.”*

No second-hop search.

<answer> 1945 ×

The two-hop structure (designer → city; city + date → mayor; mayor → birth year) admits a single-query collapse only by accident; the load-bearing decision is whether to issue a second `tavily-search` after the first hop returns. AXPO consistently issues the follow-up; all four GRPO rollouts on this question stop after the first hop and fall back to a riddle-style guess (1945, 1963, 1968, etc.).